[46]. Our present results have suggested that inhibition of Trk signals might be a useful target to normalize of tumoral vessels. An appropriate animal experiment will be needed for further examination of this possibility, and to confirm whether Trks are useful targets for anti-angiogenic and anti-lymphangiogenic therapy in OSCC.

Acknowledgment This work was supported in part by Grant-in-Aid for Scientific Research from Japan Society for the Promotion of Science, Japan.

Conflict of interest We declare that there is not any Financial Support or Relationships which may pose a conflict of interest in the contents of the submitted manuscript.

References

1. Chen YJ, Lin SC, Kao T, Chang CS, Hong PS, Shieh TM, Chang KW (2004) Genome-wide profiling of oral squamous cell carcinoma. J Pathol 204:326–332
2. Hunter KD, Parkinson EK, Harrison PR (2005) Profiling early head and neck cancer. Nat Rev Cancer 5:127–135
3. Lippman SM, Hong WK (2001) Molecular markers of the risk of oral cancer. N Engl J Med 344:1323–1326
4. Tanaka S, Sobue T (2005) Comparison of oral and pharyngeal cancer mortality in five countries: France, Italy, Japan, UK and USA from the WHO Mortality Database (1960–2000). Jpn J Clin Oncol 35:488–491
5. Hershkovich O, Oliva J, Nagler RM (2004) Lethal synergistic effect of cigarette smoke and saliva in an in vitro model: does saliva have a role in the development of oral cancer? Eur J Cancer 40:1760–1767
6. Dos Reis PP, Bharadwaj RR, Machado J, Macmillan C, Pintilie M, Sukhai MA, Perez-Ordonez B, Gullane P, Irish J, Kamel-Reid S (2008) Claudin 1 overexpression increases invasion and is associated with aggressive histological features in oral squamous cell carcinoma. Cancer 113:3169–3180
7. Thiele CJ, Li Z, McKee AE (2009) On Trk: the TrkB signal transduction pathway is an increasingly important target in cancer biology. Clin Cancer Res 15:5962–5967
8. Inoue K, Ito K, Osato M, Lee B, Bae SC, Ito Y (2007) The transcription factor Runx3 represses the neurotrophin receptor TrkB during lineage commitment of dorsal root ganglion neurons. J Biol Chem 282:24175–24184
9. Nakamura S, Senzaki K, Yoshikawa M, Nishimura M, Inoue K, Ito Y, Ozaki S, Shiga T (2008) Dynamic regulation of the expression of neurotrophin receptors by Runx3. Development 135:1703–1711
10. Sasahira T, Kurihara M, Yamamoto K, Bhawal U, Kirita T, Kuniyasu H (2011) Downregulation of runt-related transcription factor 3 (RUNX3) associated with poor prognosis of adenoid cystic and mucoepidermoid carcinomas of the salivary gland. Cancer Sci 102:492–497
11. Tessarollo L (1998) Pleiotropic functions of neurotrophins in development. Cytokine Growth Factor Rev 9:125–137
12. Yu X, Liu L, Cai B, He Y, Wan X (2008) Suppression of anoikis by the neurotrophic receptor TrkB in human ovarian cancer. Cancer Sci 99:543–552
13. Bouzas-Rodriguez J, Cabrera JR, Delloye-Bourgeois C, Ichim G, Delcros JG, Raquin MA, Rousseau R, Combaret V, Bénard J, Tauszig-Delamasure S, Mehlen P (2010) Neurotrophin-3 production promotes human neuroblastoma cell survival by inhibiting TrkC-induced apoptosis. J Clin Invest 120:850–858
14. Davidson B, Reich R, Lazarovici P, Nesland JM, Skrede M, Risberg B, Tropé CG, Flørenes VA (2003) Expression and activation of the nerve growth factor receptor TrkA in serous ovarian carcinoma. Clin Cancer Res 9:2248–2259
15. Sclabas GM, Fujioka S, Schmidt C, Li Z, Frederick WA, Yang W, Yokoi K, Evans DB, Abbruzzese JL, Hess KR, Zhang W, Fidler IJ, Chiao PJ (2005) Overexpression of tropomysin-related kinase B in metastatic human pancreatic cancer cells. Clin Cancer Res 11:440–449
16. Yang ZF, Ho DW, Lam CT, Luk JM, Lum CT, Yu WC, Poon RT, Fan ST (2005) Identification of brain-derived neurotrophic factor as a novel functional protein in hepatocellular carcinoma. Cancer Res 65:219–225
17. Satoh F, Mimata H, Nomura T, Fujita Y, Shin T, Sakamoto S, Hamada Y, Nomura Y (2001) Autocrine expression of neurotrophins and their receptors in prostate cancer. Int J Urol 8:S28–S34
18. Nakagawara A, Azar CG, Scavarda NJ, Brodeur GM (1994) Expression and function of TRK-B and BDNF in human neuroblastomas. Mol Cell Biol 14:759–767
19. Chen-Tsai CP, Colome-Grimmer M, Wagner RF Jr (2004) Correlations among neural cell adhesion molecule, nerve growth factor, and its receptors, TrkA, TrkB, TrkC, and p75, in perineural invasion by basal cell and cutaneous squamous cell carcinomas. Dermatol Surg 30:1009–1016
20. Nakagawara A, Arima-Nakagawara M, Scavarda NJ, Azar CG, Cantor AB, Brodeur GM (1993) Association between high levels of expression of the TRK gene and favorable outcome in human neuroblastoma. N Engl J Med 328:847–854
21. Yamashiro DJ, Nakagawara A, Ikegaki N, Liu XG, Brodeur GM (1996) Expression of TrkC in favorable human neuroblastomas. Oncogene 12:37–41
22. Segal RA, Goumnerova LC, Kwon YK, Stiles CD, Pomeroy SL (1994) Expression of the neurotrophin receptor TrkC is linked to a favorable outcome in medulloblastoma. Proc Natl Acad Sci USA 91:12867–12871
23. Sasahira T, Oue N, Kirita T, Luo Y, Bhawal UK, Fujii K, Yasui W, Kuniyasu H (2008) Reg IV expression is associated with cell growth and prognosis of adenoid cystic carcinoma in the salivary gland. Histopathology 53:667–675
24. Li QL, Ito K, Sakakura C, Fukamachi H, Inoue K, Chi XZ, Lee KY, Nomura S, Lee CW, Han SB, Kim HM, Kim WJ, Yamamoto H, Yamashita N, Yano T, Ikeda T, Itohara S, Inazawa J, Abe T, Hagiwara A, Yamagishi H, Ooe A, Kaneda A, Sugimura T, Ushijima T, Bae SC, Ito Y (2002) Causal relationship between the loss of RUNX3 expression and gastric cancer. Cell 109:113–124
25. Sasaki T, Fujii K, Yoshida K, Shimura H, Sasahira T, Ohmori H, Kuniyasu H (2006) Peritoneal metastasis inhibition by linoleic acid with activation of PPARγ in human gastrointestinal cancer cells. Virchows Arch 448:422–427
26. Sasaki T, Shimura H, Sasahira T, Fujii K, Kuniyasu H (2005) High concentration of deoxycholic acid abrogates in vitro transformation of IEC6 intestinal cells by azoxymethane. J Exp Clin Cancer Res 24:625–631
27. Sasahira T, Akama Y, Fujii K, Kuniyasu H (2005) Expression of receptor for advanced glycation end products and HMGB1/amphoterin in colorectal adenomas. Virchows Arch 446:411–415
28. Allred DC, Harvey JM, Berardo M, Clark GM (1998) Prognostic and predictive factors in breast cancer by immunohistochemical analysis. Mod Pathol 11:155–168
29. Sasahira T, Kirita T, Oue N, Bhawal UK, Yamamoto K, Fujii K, Yasui W, Kuniyasu H (2008) High mobility group box-1-inducible melanoma inhibitory activity is associated with nodal

metastasis and lymphangiogenesis in oral squamous cell carcinoma. Cancer Sci 99:1806–1812
30. Sasahira T, Kirita T, Bhawal UK, Ikeda M, Nagasawa A, Yamamoto K, Kuniyasu H (2007) The expression of receptor for advanced glycation end products is associated with angiogenesis in human oral squamous cell carcinoma. Virchows Arch 450:287–295
31. Sasahira T, Kirita T, Kurihara M, Yamamoto K, Bhawal UK, Bosserhoff AK, Kuniyasu H (2010) MIA-dependent angiogenesis and lymphangiogenesis are closely associated with progression, nodal metastasis and poor prognosis in tongue squamous cell carcinoma. Eur J Cancer 46:2285–2294
32. Nakamura K, Martin KC, Jackson JK, Beppu K, Woo CW, Thiele CJ (2006) Brain-derived neurotrophic factor activation of TrkB induces vascular endothelial growth factor expression via hypoxia-inducible factor-1alpha in neuroblastoma cells. Cancer Res 66:4249–4255
33. Tacconelli A, Farina AR, Cappabianca L, Desantis G, Tessitore A, Vetuschi A, Sferra R, Rucci N, Argenti B, Screpanti I, Gulino A, Mackay AR (2004) TrkA alternative splicing: a regulated tumor-promoting switch in human neuroblastoma. Cancer Cell 6:347–360
34. Cristofaro B, Stone OA, Caporali A, Dawbarn D, Ieronimakis N, Reyes M, Madeddu P, Bates DO, Emanueli C (2010) Neurotrophin-3 is a novel angiogenic factor capable of therapeutic neovascularization in a mouse model of limb ischemia. Arterioscler Thromb Vasc Biol 30:1143–1150
35. Brzezianska E, Pastuszak-Lewandoska D, Lewinski A (2007) Rearrangements of NTRK1 oncogene in papillary thyroid carcinoma. Neuro Endocrinol Lett 28:221–229
36. McGregor LM, McCune BK, Graff JR, McDowell PR, Romans KE, Yancopoulos GD, Ball DW, Baylin SB, Nelkin BD (1999) Roles of trk family neurotrophin receptors in medullary thyroid carcinoma development and progression. Proc Natl Acad Sci USA 96:4540–4545
37. Riedel F, Gotte K, Bergler W, Hormann K (2001) Inverse correlation of apoptotic and angiogenic markers in squamous cell carcinoma of the head and neck. Oncol Rep 8:471–476
38. Larcher F, Robles AI, Duran H, Murillas R, Quintanilla M, Cano A, Conti CJ, Jorcano JL (1996) Up-regulation of vascular endothelial growth factor/vascular permeability factor in mouse skin carcinogenesis correlates with malignant progression state and activated H-ras expression levels. Cancer Res 56:5391–5396
39. Li Z, Jaboin J, Dennis PA, Thiele CJ (2005) Genetic and pharmacologic identification of Akt as a mediator of brain-derived neurotrophic factor/TrkB rescue of neuroblastoma cells from chemotherapy-induced cell death. Cancer Res 65:2070–2075
40. Jin W, Yun C, Kwak MK, Kim TA, Kim SJ (2007) TrkC binds to the type II TGF-beta receptor to suppress TGF-beta signaling. Oncogene 26:7684–7691
41. Hanai J, Chen LF, Kanno T, Ohtani-Fujita N, Kim WY, Guo WH, Imamura T, Ishidou Y, Fukuchi M, Shi MJ, Stavnezer J, Kawabata M, Miyazono K, Ito Y (1999) Interaction and functional cooperation of PEBP2/CBF with Smads. Synergistic induction of the immunoglobulin germline Calpha promoter. J Biol Chem 274:31577–31582
42. Zaidi SK, Sullivan AJ, van Wijnen AJ, Stein JL, Stein GS, Lian JB (2002) Integration of Runx and Smad regulatory signals at transcriptionally active subnuclear sites. Proc Natl Acad Sci USA 99:8048–8053
43. Chuang LS, Ito Y (2010) RUNX3 is multifunctional in carcinogenesis of multiple solid tumors. Oncogene 9:2605–2615
44. Tsunematsu T, Kudo Y, Iizuka S, Ogawa I, Fujita T, Kurihara H, Abiko Y, Takata T (2009) RUNX3 has an oncogenic role in head and neck cancer. PLoS ONE 4:e5892
45. Jain RK, Munn LL, Fukumura D (2002) Dissecting tumour pathophysiology using intravital microscopy. Nat Rev Cancer 2:266–276
46. Jain RK (2005) Normalization of tumor vasculature: an emerging concept in antiangiogenic therapy. Science 307:58–62

Increased Phosphorylation of AKT in High-risk Gastric Mucosa

TAKAMITSU SASAKI[1], HIROKI KUNIYASU[2], YI LUO[2], MISAHO KITAYOSHI[2], ERIKO TANABE[2], DAISUKE KATO[1], SATOSHI SHINYA[1], KIYOMU FUJII[2], HITOSHI OHMORI[2] and YUICHI YAMASHITA[1]

[1]*Department of Gastroenterolgical Surgery, Fukuoka University School of Medicine, Fukuoka, Japan;*
[2]*Department of Molecular Pathology, Nara Medical University, Kashihara, Japan*

Abstract. *Aim: To establish the role of oxidative stress and v-akt murine thymoma viral oncogene homolog (AKT) activation in gastric cancer development, we examined the levels of phosphorylated AKT (pAKT), inducible nitric oxide synthase (iNOS), nitrotyrosine (NT), and human telomerase reverse transcriptase (hTERT) by enzyme-linked immunosorbent assay in 73 non-cancerous gastric mucosa and 10 gastric carcinomas. We found that the levels of pAKT were associated with the levels of iNOS, NT, and hTERT. Gastric mucosa was classified into four categories: chronic gastritis without Helicobacter pylori (CG), chronic active gastritis with H. pylori (CAG), chronic metaplastic gastritis without H. pylori (CMG), and chronic gastritis with atypia without H. pylori (CGA). We found increasing levels of pAKT, iNOS, and NT in the order of CG, CAG, CMG, and CGA. hTERT was detected only in CGA. These findings suggest that oxidative stress might be associated with AKT activation and hTERT induction and that mucosa in CGA might confer a high-risk status for gastric carcinogenesis.*

v-Akt murine thymoma viral oncogene homolog (AKT) is a pivotal regulator of cell survival, proliferation, and differentiation. It is a member of the phosphatidylinositol-3 kinase (PI3K) signaling pathway. Stimulation of receptor tyrosine kinases or G-proteins activates PI3K, which in turn activates AKT. AKT phosphorylation is maintained by heat-shock protein-90, and AKT is dephosphorylated by protein phosphatase-2A. AKT regulates signaling *via* various growth factors and cytokines. In particular, activation of insulin-like growth factor-1 receptor, epidermal growth factor receptor, and human epidermal growth factor receptor-2, which are important in cancer progression, activate AKT (3, 15). AKT is also a biomarker that predicts metastasis of human gastrointestinal cancer (11).

Phosphorylation of AKT modulates signals by phosphatase, tensin homolog deleted on chromosome 10 (PTEN), and the mammalian target of rapamycin (mTOR), resulting in diverse effects on cells (4). In this regard, AKT1 is recognized as an apoptotic inhibitor, which contributes to cancer progression. Phosphorylation *via* AKT inactivates B-cell lymphoma-2 (BCL-2) antagonist of cell death resulting in its dissociation from BCL-2. In addition, AKT activates nuclear factor (NF)-κB, which in turn up-regulates transcription of many survival genes (6). AKT also promotes angiogenesis through up-regulation of vascular endothelial growth factor (12). The activation and expression of AKT promote tumorigenesis, thus AKT represents a relevant molecular target for cancer treatment (3).

In the present study, alteration of AKT phosphorylation in gastric mucosa and the role of oxidative stress in AKT phosphorylation were examined for the evaluation of high-risk gastric mucosa.

Materials and Methods

Cell culture and reagents. The human gastric cancer cell line MKN28 (kindly donated by Professor Wataru Yasui, Hiroshima University, Japan) was maintained in Dulbecco's modified essential medium (Sigma Chemical Co., St. Louis, MO, USA) containing 10% fetal bovine serum (Sigma Chemical Co.) at 5% CO_2 in air and 37°C.

Clinical materials. Eighty-three biopsied gastric tissue samples obtained from patients histologically-diagnosed at the Department of Molecular Pathology, Nara Medical University, were examined. One half of each tissue specimen was used for pathological diagnosis and the other half was used for enzyme-linked immunosorbent assay (ELISA). The tissues had been frozen quickly in liquid nitrogen and stored at –80°C. Seventy-three of the tissue samples were obtained from non-cancerous cases were classified into four categories: [i] Chronic gastritis without *Helicobacter pylori* (CG); [ii] chronic active gastritis with *H. pylori* (CAG): chronic gastritis with regenerative epithelial change and polymorphonuclear cell infiltration in the mucosa; [iii] chronic metaplastic gastritis without *H. pylori* (CMG):

Correspondence to: Hiroki Kuniyasu, at Department of Molecular Pathology, Nara Medical University, 840 Shijo-cho, Kashihara, Nara, 634-8521, Japan. Tel: +81 744223051, Fax: +81 744257308, e-mail: cooninh@zb4.so-net.ne.jp

Key Words: AKT, hTERT, iNOS, oxidative stress.

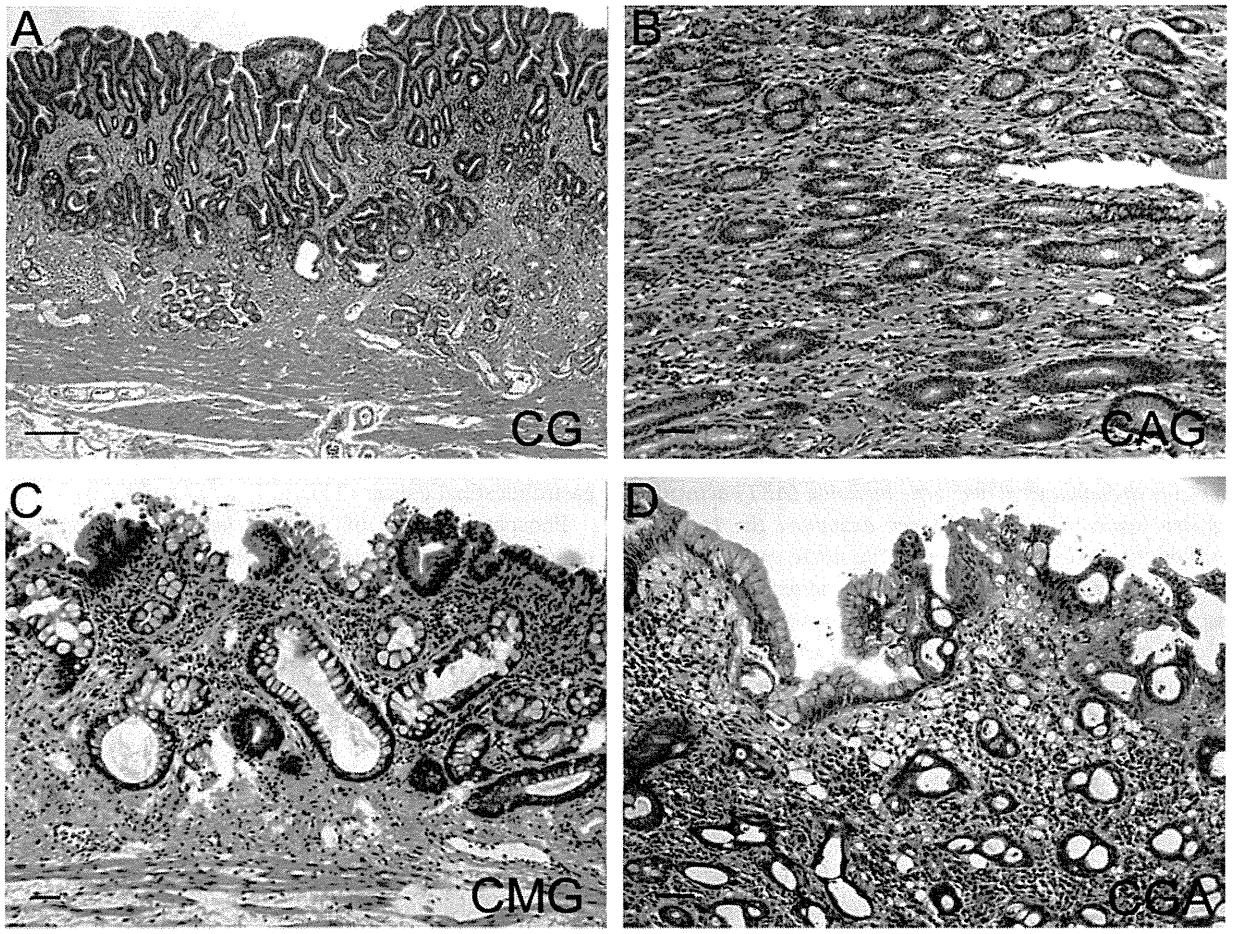

Figure 1. *Histopathological findings of the gastric mucosa (hematoxylin and eosin staining). A: Chronic gastric mucosa without Helicobacter pylori infection (CG). B: Chronic active gastritis with H. pylori infection (CAG). C: Chronic metaplastic gastritis without H. pylori (CMG). D: Chronic gastritis with atypia (CGA). Bar=100 μm.*

atrophic mucosa with diffuse intestinal metaplasia; and [iv] chronic gastritis with atypia without *H. pylori* (CGA): chronic gastritis with regenerative change and nuclear swelling, chromatin increment, or nucleoli formation (nuclear atypia). Ten of the tissues were adenocarcinomas diagnosed as papillary adenocarcinoma (n=3) or well-differentiated tubular adenocarcinoma (n=7). The diagnosis was performed by two pathologists (H.K. and H.O.).

ELISA. The levels of pAKT, TERT, nitrotyrosine (NT), and inducible nitric oxide synthase (iNOS) were determined using specific ELISA kits according to the manufacturer instructions: AKT (pS473) ELISA kit (Abcam, Cambridge, UK), human telomerase reverse transcriptase (HTERT) ELISA kit (Oxford Expression Technology, Oxford, UK) (14), ELISA for nitrotyrosine (Hycult Biotechnology BV, Uden, the Netherlands) (5) and CytoGLOW iNOS Colorimetric Cell-Based ELISA kit (Assay Biotechnology Co. Inc., Sunnyvale, CA), respectively. Whole-tissue lysates were extracted from liquid nitrogen-frozen tumor materials using a lysis buffer (9). ELISA was performed in triplicate.

Nitrite. Sodium nitroprusside (SNP) was used as a NO donor using concentrations designated in the results section. NO concentration was detected as a nitrite concentration, which was measured using the Griess method. Cultured medium was mixed with an equal amount of Griess solution (1% sulfanilamide, 0.1% naphthylethylenediamine dihydrochloride, 2.5% phosphoric acid), and OD540 was measured 10 minutes after incubation. Nitrite concentration was determined on the basis of a standard curve generated using different concentrations of sodium nitrite.

Statistical analysis. Statistical analyses of experimental data were performed using Spearman's r and analysis of variance (InStat; Graphpad Software Inc., La Jolla, CA, USA). Statistical significance was defined as a two-sided *p*-value of less than 0.05.

Results

Histological classification of gastric mucosa. In the present study, the gastric mucosa status was classified into four categories; CG, CAG, CMG, and CGA (Figure 1). On the basis of the *H. pylori* infection status, temporal alteration of gastric mucosa is reflected in CG, CAG, and CMG.

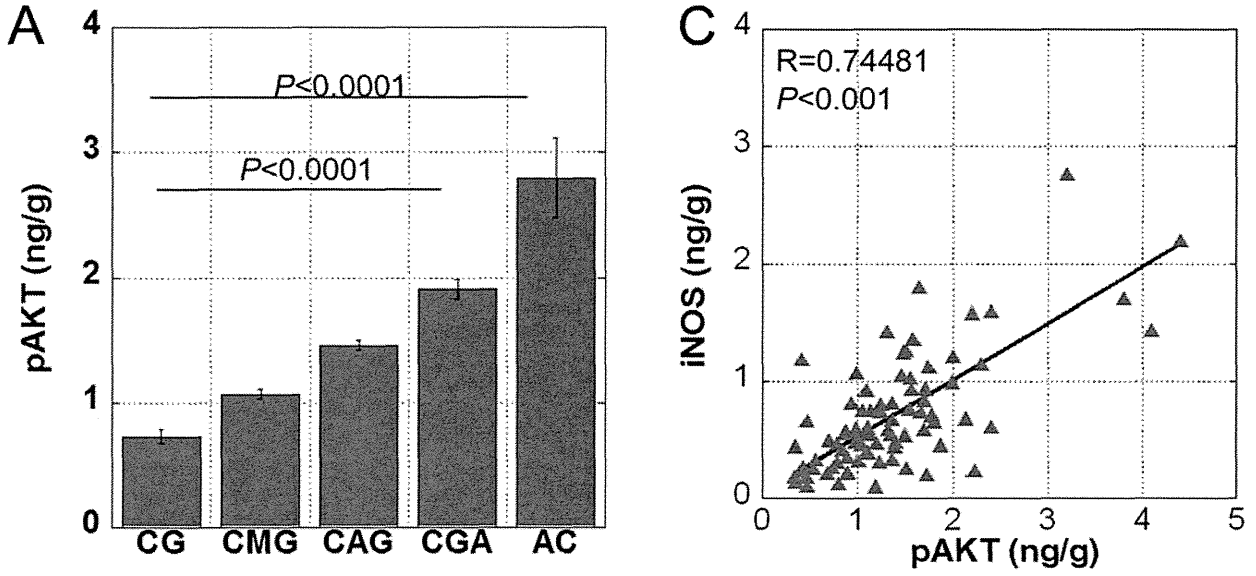

Figure 2. *Phosphorylated v-akt murine thymoma viral oncogene homolog (AKT) level and the association with inducible nitric oxide synthase (iNOS) expression. The level of pAKT (A) and iNOS (B) were examined by enzyme-linked immunosorbent assay. The relationship between pAKT and iNOS was compared by Spearman's correlation analysis (C). Error bar=SE. CG: Chronic gastric mucosa without Helicobacter pylori infection, CAG: chronic active gastritis with H. pylori infection, CMG: chronic metaplastic gastritis without H. pylori, CGA: chronic gastritis with atypia. Levels of pAKT and iNOS increased from CG to CMG to CAG to CGA (A, B). Levels of pAKT and iNOS were significantly correlated (C).*

Levels of pAKT and iNOS in gastric mucosa. As shown in Figure 2A, the level of pAKT gradually increased in the order of CG, CMA, CAG, and CGA. The level of pAKT in CGA was 2.6-times higher than in samples classified as CG.

iNOS is responsible for the production of NO and mediates oxidative stress in the gastric mucosa. Similarly to pAKT, the level of iNOS increased in the order of CG, CMG, CAG and CGA (Figure 2B). Because NO has been shown to up-regulate the level of pAKT, we examined the relationship between pAKT and iNOS. As shown in Figure 2C, we found a significant correlation ($p<0.001$) between the levels of pAKT and iNOS.

Levels of pAKT and NT in gastric mucosa. The level of NT increased in the order of CG, CMG, CAG and CGA (Figure 3A) and level were correlated with the level of pAKT (Figure 3B).

Levels of pAKT and hTERT in gastric mucosa. We have already reported that AKT activation is associated with hTERT activation. Among the four mucosal categories, only samples of CGA exhibited hTERT expression, albeit at lower levels than those of cancer cases (Figure 4A). The levels of hTERT were correlated with the levels of pAKT in the analysis of all patients (Figure 4B).

Nitric oxide induces AKT phosphorylation. Data obtained from clinical samples suggested that NO induces AKT phosphorylation. Therefore, we examined the effect of NO on AKT phosphorylation in gastric epithelial cells. Primary cultured gastric mucosal cells were treated with different concentrations of SNP, a NO donor, and the levels of AKT and pAKT were examined. As shown in Figure 5, the levels of pAKT were significantly increased by SNP treatment in CGA samples and in MKN28 cancer cells but not in CG, CAG, or CMG.

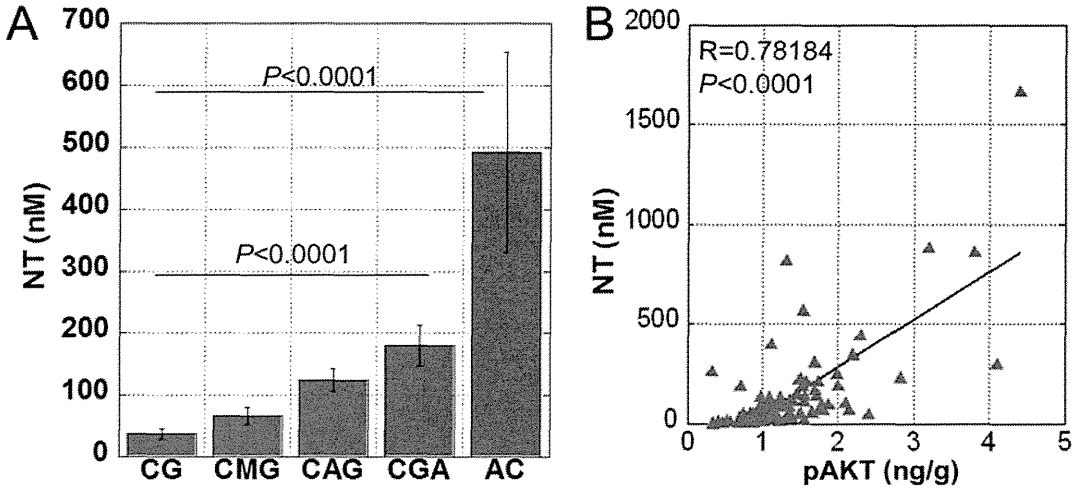

Figure 3. *Nitrotyrosine (NT) level and association with phosphorylated v-akt murine thymoma viral oncogene homolog (AKT) expression. The level of NT was examined by enzyme-linked immunosorbent assay (A). The relationship between NT and pAKT was compared using Spearman correlation analysis (B). Error bar=SE. CG: Chronic gastric mucosa without Helicobacter pylori infection, CAG: chronic active gastritis with H. pylori infection, CMG: chronic metaplastic gastritis without H. pylori, CGA: chronic gastritis with atypia. The levels of NT increased from CG to CMG to CAG to CGA (A) and were correlated with the levels of pAKT (B).*

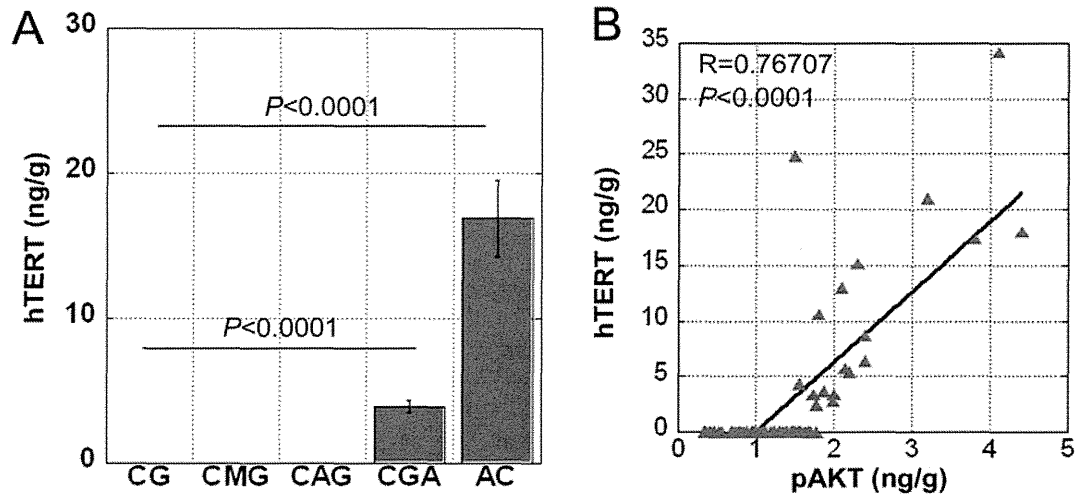

Figure 4. *human telomerase reverse transcriptase (hTERT) level and the association with phosphorylated v-akt murine thymoma viral oncogene homolog (AKT) expression. The level of hTERT was examined by enzyme-linked immunosorbent assay (A). The relationship between hTERT and pAKT was compared using Spearman correlation analysis (B). Error bar=SE. CG: Chronic gastric mucosa without Helicobacter pylori infection, CAG: chronic active gastritis with H. pylori infection, CMG: chronic metaplastic gastritis without H. pylori, CGA: chronic gastritis with atypia. Among the 4 mucosal categories, only CGA samples showed hTERT expression (A). Levels of hTERT were correlated with the levels of pAKT (B).*

Discussion

Our data showed that AKT phosphorylation was associated with the expressions of iNOS and hTERT and with increased level of NT. The levels of pAKT, iNOS, NT, and hTERT were increased in CGA, which is considered to be a high-risk status for gastric carcinogenesis.

In gastric mucosal pathology, *H. pylori* plays a pivotal role, because it induces chronic inflammation and increases the production of reactive oxygen species. *H. pylori* stimulates proliferation of gastric mucosal cells *via* type-IV secretion of CagA followed by its phosphorylation by Schmidt-Ruppin A-2 avian sarcoma viral oncogene (src) homology 2 domain-containing protein tyrosine phosphatase-

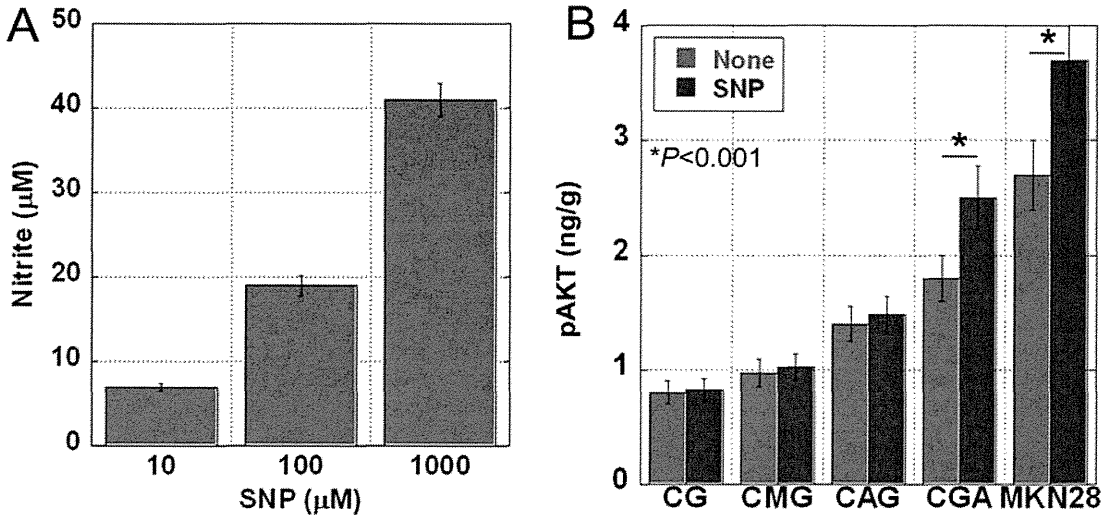

Figure 5. *Phosphorylation of v-akt murine thymoma viral oncogene homolog (AKT) by nitric oxide (NO) in gastric mucosa. A: The levels of nitrite generated by the treatment of cells with the NO donor sodium nitroprusside (SNP). B: Fresh-tissue biopsies (n=3 in each category) were incubated with SNP (100 μM) and the level of pAKT was determined by enzyme-linked immunosorbent assay. MKN28 cells are transformed gastric cells. Error bar, SD. CG: Chronic gastric mucosa without Helicobacter pylori infection, CAG: chronic active gastritis with H. pylori infection, CMG: chronic metaplastic gastritis without H. pylori, CGA: chronic gastritis with atypia. Levels of pAKT were increased by SNP treatment in CGA samples and in MKN28 cancer cells but not in CG, CAG, or CMG.*

2 (SHP2) (7, 8). CagA activates SHP2 phosphatase, which inhibits signal transducers and activators of transcription (STAT)-mediated growth-suppressive signal and activates extracellular signal-regulated kinase (ERK)-mediated growth signal (16). The increased growth activity might enhance the risk of gene alteration.

We classified the status of gastric mucosa according to inflammation and immortalization by hTERT expression. Since AKT is a key protein that links inflammation and tumorigenesis, it is the focus of our study. iNOS is a significant mediator of inflammation in the gastric mucosa. Increased expression of iNOS is epigenetically induced by *H. pylori* infection as a host defense (1). NT is a marker of NO-induced protein degradation. We examined the expression of iNOS and NT to evaluate inflammation and the expression of hTERT as a marker of immortality. Our data showed that the levels of pAKT were associated with hTERT expression in CGA. Our previous study showed that pAKT levels were associated with hTERT expression in gastric adenocarcinomas (14). These findings suggest that the immortality of gastric mucosal cells maybe associated with inflammation-induced AKT activation.

Our results demonstrated that the levels of iNOS and NT were associated with pAKT (13). pAKT, iNOS, and NT were higher in CAG, CMG, and CGA. Interestingly, high pAKT level in CAG associated with *H. pylori*-induced active inflammation. In contrast, increased pAKT in CMG suggests that persistent iNOS up-regulation develops during the metaplastic process. The highest pAKT level in CGA might develop during carcinogenic processes (10). *In vitro* analysis showed that only CGA and MKN28 cancer cells exhibited up-regulation of pAKT in response to short exposure to NO. In Barrett esophagus, activation of AKT is associated with the dysplasia–carcinoma sequence (2). Moreover, only CGA mucosa expressed hTERT. These findings suggest that CGA is likely to be a distinct category in the process of gastric carcinogenesis.

Our data suggest that CGA should be viewed as high-risk mucosa for gastric cancer and that patients with CGA should be evaluated by further endoscopic and histopathological methods.

References

1 Angrisano T, Lembo F, Peluso S, Keller S, Chiariotti L and Pero R: *Helicobacter pylori* regulates iNOS promoter by histone modifications in human gastric epithelial cells. Med Microbiol Immunol *201*: 249-257, 2012.

2 Beales IL, Ogunwobi O, Cameron E, El-Amin K, Mutungi G and Wilkinson M: Activation of AKT is increased in the dysplasia-carcinoma sequence in Barrett's oesophagus and contributes to increased proliferation and inhibition of apoptosis: A histopathological and functional study. BMC Cancer *7*: 97, 2007.

3 Berg M and Soreide K: EGFR and downstream genetic alterations in KRAS/BRAF and PI3K/AKT pathways in colorectal cancer: Implications for targeted therapy. Discov Med *14*: 207-214, 2012.

4 Cheung M and Testa JR: Diverse mechanisms of AKT pathway activation in human malignancy. Curr Cancer Drug Targets *13(3)*: 234-244, 2013.

5 Chihara Y, Fujimoto K, Kondo H, Moriwaka Y, Sasahira T, Hirao Y, and Kuniyasu H: Antitumor effects of liposome-encapsulated titanium dioxide in nude mice. Pathobiology *74*: 353-358, 2007.
6 Downward J: PI-3-kinase, AKT and cell survival. Semin Cell Dev Biol *15*: 177-182, 2004.
7 Hatakeyama M: Oncogenic mechanisms of the *Helicobacter pylori* CagA protein. Nat Rev Cancer *4*: 688-694, 2004.
8 Higashi H, Tsutsumi R, Muto S, Sugiyama T, Azuma T, Asaka M and Hatakeyama M: SHP-2 tyrosine phosphatase as an intracellular target of *Helicobacter pylori* CagA protein. Science 295: 683-686, 2002.
9 Kuniyasu H, Luo Y, Fujii K, Sasahira T, Moriwaka Y, Tatsumoto N, Sasaki T, Yamashita Y and Ohmori H: CD10 enhances metastasis of colorectal cancer by abrogating the antitumoural effect of methionine-enkephalin in the liver. Gut *59*: 348-356, 2010.
10 Murata M, Thanan R, Ma N and Kawanishi S: Role of nitrative and oxidative DNA damage in inflammation-related carcinogenesis. J Biomed Biotechnol *2012*: ID623019, 2012. (free PMC article)
11 Ng L, Poon RT and Pang R: Biomarkers for predicting future metastasis of human gastrointestinal tumors. Cell Mol Life Sci.
12 Radisavljevic Z: AKT as locus of cancer angiogenic robustness and fragility. J Cell Physiol *228*: 21-24, 2013.
13 Ridnour LA, Barasch KM, Windhausen AN, Dorsey TH, Lizardo MM, Yfantis HG, Lee DH, Switzer CH, Cheng RY, Heinecke JL, Brueggemann E, Hines HB, Khanna C, Glynn SA, Ambs S and Wink DA: Nitric oxide synthase and breast cancer: role of TIMP-1 in NO-mediated AKT activation. PLoS One *7*: e44081, 2012.
14 Sasaki T, Kuniyasu H, Luo Y, Kitayoshi M, Tanabe E, Kato D, Shinya S, Fujii K, Ohmori H and Yamashita Y: AKT activation and telomerase reverse transcriptase expression are concurrently associated with prognosis of gastric cancer. Pathobiology, in press.
15 Sukawa Y, Yamamoto H, Nosho K, Kunimoto H, Suzuki H, Adachi Y, Nakazawa M, Nobuoka T, Kawayama M, Mikami M, Matsuno T, Hasegawa T, Hirata K, Imai K and Shinomura Y: Alterations in the human epidermal growth factor receptor 2-phosphatidylinositol 3-kinase-v-AKT pathway in gastric cancer. World J Gastroenterol *18*: 6577-6586, 2012.
16 You M, Yu DH and Feng GS: SHP-2 tyrosine phosphatase functions as a negative regulator of the interferon-stimulated JAK/STAT pathway. Mol Cell Biol *19*: 2416-2424, 1999.

Received June 3, 2013
Revised June 24, 2013
Accepted June 26, 2013

Published OnlineFirst November 6, 2013; DOI: 10.1158/0008-5472.CAN-13-1052

Cancer Research

Cancer Usurps Skeletal Muscle as an Energy Repository

Yi Luo, Junya Yoneda, Hitoshi Ohmori, et al.

Cancer Res 2014;74:330-340. Published OnlineFirst November 6, 2013.

Published OnlineFirst November 6, 2013; DOI: 10.1158/0008-5472.CAN-13-1052

Tumor and Stem Cell Biology

Cancer Research

Cancer Usurps Skeletal Muscle as an Energy Repository

Yi Luo[1], Junya Yoneda[2], Hitoshi Ohmori[1], Takamitsu Sasaki[3], Kazutaka Shimbo[2], Sachise Eto[2], Yumiko Kato[2], Hiroshi Miyano[2], Tsuyoshi Kobayashi[2], Tomonori Sasahira[1], Yoshitomo Chihara[1], and Hiroki Kuniyasu[1]

Abstract

Cancer cells produce energy through aerobic glycolysis, but contributions of host tissues to cancer energy metabolism are unclear. In this study, we aimed to elucidate the cancer–host energy production relationship, in particular, between cancer energy production and host muscle. During the development and progression of colorectal cancer, expression of the secreted autophagy-inducing stress protein HMGB1 increased in the muscle of tumor-bearing animals. This effect was associated with decreased expression of pyruvate kinase PKM1 and pyruvate kinase activity in muscle via the HMGB1 receptor for advanced glycation endproducts (RAGE). However, muscle mitochondrial energy production was maintained. In contrast, HMGB1 addition to colorectal cancer cells increased lactate fermentation. In the muscle, HMGB1 addition induced autophagy by decreasing levels of active mTOR and increasing autophagy-associated proteins, plasma glutamate, and ^{13}C-glutamine incorporation into acetyl-CoA. In a mouse model of colon carcinogenesis, a temporal increase in HMGB1 occurred in serum and colonic mucosa with an increase in autophagy associated with altered plasma free amino acid levels, increased glutamine, and decreased PKM1 levels. These differences were abolished by administration of an HMGB1 neutralizing antibody. Similar results were obtained in a mouse xenograft model of human colorectal cancer. Taken together, our findings suggest that HMGB1 released during tumorigenesis recruits muscle to supply glutamine to cancer cells as an energy source. *Cancer Res; 74(1); 330–40. ©2013 AACR.*

Introduction

Nontransformed mammalian cells produce energy via the tricarboxylic acid (TCA) cycle and the electron transport system in the presence of oxygen. In contrast, transformed cells produce energy through lactate fermentation, mainly in the presence of oxygen, which is called the Warburg effect (1). Recently, the Warburg effect has been shown to result from a switch in the expression of pyruvate kinase (PK) isoforms (2, 3). Activation of cellular myelocytomatosis (c-Myc) changes the alternative splicing pattern from *PKM1* to *PKM2*, and then inactivation of PKM2 via phosphorylation induces anaerobic energy production (4–6). Energy production in cancer-burdened hosts and the relationship between host and cancer remain unclear. Patients with advanced cancer show malnutrition, weight loss, and cachexia, which suggests that cancer affects the energy production pathways of the host. To increase tolerance to anticancer treatments and improve the quality of life for patients with cancer, it is important to elucidate the altered energy production mechanisms in cancer-burdened hosts.

Free amino acids in plasma are supplied by dietary proteins and proteolysis (7, 8); therefore, alterations in the amino acids in plasma reflect changes in metabolism. Proteolysis is driven by ubiquitin-proteasomal degradation and autophagic-lysosomal degradation, and the latter is responsible for bulk proteolysis (9). mTOR is a key molecule controlling autophagy (10). Inactivation of the mTOR complex by genotoxic stress, starvation, p53, or AMP-activated protein kinase induces activation of the autophagy machinery, including beclin-1, autophagy-related genes, and the microtubule-associated protein light chain (LC) 3. The plasma free amino acid (PFAA) profile is affected by various pathologic conditions. Japanese patients with metabolic syndrome have altered PFAA profiles; however, reduction of body mass index, blood pressure, and hemoglobin A1c and triglyceride levels was shown to normalize the profile (11). Patients with cancer of the lung, stomach, colorectum, breast, and prostate show altered PFAA profiles (12, 13). The pattern and degree of the changes depend on the type of cancer. Determination of the precise mechanism underlying alterations in the PFAA profile is required to utilize the profile data for disease diagnosis and treatment.

HMGB1 is a multifunctional protein that functions as a growth factor and enhances proliferation, invasion, and metastasis by binding to receptor for advanced glycation endproducts

Authors' Affiliations: [1]Department of Molecular Pathology, Nara Medical University, Shijo-cho, Kashihara; [2]Institute for Innovation Ajinomoto Co., Inc., Suzuki-cho, Kawasaki; and [3]Department of Gastrointestinal Surgery, Fukuoka University School of Medicine, Nanakuma, Minami-ku, Fukuoka, Japan

Note: Supplementary data for this article are available at Cancer Research Online (http://cancerres.aacrjournals.org/).

Corresponding Author: Hiroki Kuniyasu, Department of Molecular Pathology, Nara Medical University, 840 Shijo-cho, Kashihara, Nara 634-8521, Japan. Phone: 81-744-22-3051; Fax: 81-744-25-7308; E-mail: cooninh@zb4.so-net.ne.jp

doi: 10.1158/0008-5472.CAN-13-1052

Published OnlineFirst November 6, 2013; DOI: 10.1158/0008-5472.CAN-13-1052

(RAGE) in cancers (14, 15). HMGB1 is released by necrotic cells and secreted from monocyte-lineage cells, and induces inflammation (16, 17). An excess of HMGB1 induces apoptosis in monocyte-lineage cells, which reduces anticancer immunity and enhances cancer metastasis (15). HMGB1 also plays a pivotal role in the carcinogenesis and progression of colorectal cancer (18–20). In a rat colon carcinogenesis model using azoxymethane, HMGB1 levels continuously increased in the colonic mucosa (20). Several reports have shown that HMGB1 activates autophagy. HMGB1 binds to Toll-like receptor (TLR)-4 to activate innate immunity and immunologic autophagy by activating beclin-1 via dissociation from B-cell leukemia/lymphoma (Bcl)-2 (21, 22). Cytosolic HMGB1 also directly interacts with beclin-1 to dissociate it from Bcl-2 (23).

In the present study, we report a new cancer–host energy metabolism relationship. Cancer cell-secreted HMGB1 affects host energy metabolism in colon cancer, resulting in an altered PFAA profile with increased glutamine, which is utilized as an energy source by cancer cells.

Materials and Methods

Clinical cases

Serum samples were obtained from 46 patients with colorectal cancer who were diagnosed in the Department of Molecular Pathology at Nara Medical University (Kashihara, Nara, Japan).

Cell culture and reagents

A mouse colon cancer cell line, CT26, was kindly provided by Professor I.J. Fidler (MD Anderson Cancer Center, Houston, TX), and a human colon cancer cell line HT29 (Dainihon Pharmacy) was maintained in RPMI-1640 (Sigma) containing 10% FBS (Sigma) in 5% CO_2 in air at 37°C. Cell morphology was evaluated daily by microscopic examination. Each cell line was routinely tested for mycoplasma contamination by genomic PCR. Before article submission, each cell line was tested for Trypan blue exclusion viability and hepatitis B virus (HBV) and hepatitis C virus (HCV) infection by genomic PCR. Viability was 97.00%. The results of mycoplasma, HBV, and HCV infection testing were negative.

Recombinant human HMGB1 and anti-HMGB1 antibodies (R&D Systems), or 3-methyladenine (3MA), p38 inhibitor (SB239063), and 6-diazo-S-oxo-L-norleucine (DON; Sigma) were purchased.

Animal models

BALB/c and C57BL/6 male mice (Japan SLC) were maintained according to the institutional guidelines approved by the Committee for Animal Experimentation of Nara Medical University, and in accordance with the current regulations and standards established by the Ministry of Health, Labor, and Welfare.

For the colon carcinogenesis model, 5-week-old male C57BL/6 mice were injected intraperitoneally (i.p.) with 1,2-dimethylhydrazine (DMH; 40 mg/kg body weight; Wako Chemicals) once a week for 10 weeks. For the control, PBS was injected. For neutralization of serum HMGB1, an anti-HMGB1 antibody (R&D) was intraperitoneally administered (5 μg) twice a week for 4 weeks.

For the *ex vivo* soleus muscle model, 5-week-old male BALB/c mice were euthanized by cervical dislocation. The soleus muscles were cut using a razor blade to obtain thin slices ($5 \times 5 \times 0.5$ mm^3). The slices were cultured in regular medium.

For the subcutaneous tumor model, CT26 or HT29 cancer cells (10^7 cells) were inoculated into the scapular tissue of BALC/c or nude mice.

For the *in vivo* ^{13}C-glutamine uptake model, BALB/c mice were repeatedly fasted to enhance ^{13}C-glutamine uptake by muscles (24; Fig. 5A). After each period of fasting, ^{13}C-glutamine (18 μmol/kg body weight) was injected intraperitoneally. In another BALB/c mouse, a subcutaneous tumor of CT26 cells formed. After five fasting cycles (4-hour fasting, 8-hour feeding), a $5 \times 5 \times 5$ mm^3 section of tissue was cut from the tumor and used to inoculate the scapular subcutaneous tissue of the ^{13}C-glutamine–injected mice. Anti-HMGB1 antibody (5 μg), DON (1 mg/kg body weight; ref. 25), or anti-glutaminase miRNA-liposomes were administered intraperitoneally three times a week.

Amino acid profile

Mice blood samples were obtained by cardiocentesis, mixed with ethylenediaminetetraacetic acid disodium salt (WAKO), and immediately cooled on ice. Plasma was separated by centrifugation at 3,000 rpm for 15 minutes at 4°C. The plasma samples were deproteinized in a final concentration of 50% acetonitrile. Muscle samples immediately frozen in liquid nitrogen were disrupted using a Multi-Beads Shocker (Yasui-kikai), and homogenized in extraction solution (80% methanol with phenyl-d5-alanine as an internal standard for sample preparation). The samples added with water and chloroform were centrifuged for 30 minutes at 4°C. Free amino acids were extracted from the water layer. The amino acid concentration in plasma and tissue samples were quantified as described previously (26) with minor modifications. An Inertsil C8-3 column (GL Science) was used for separation, and the mobile phase consisted of eluent A (25 mmol/L ammonium formate in water) and eluent B (water:acetonitrile = 40:60).

Immunoblot analysis and immunoprecipitation

Whole-cell lysates were prepared as described previously (27). Lysates (50 μg) or total immunoprecipitates were separated by 12.5% SDS-PAGE, and electrotransferred onto nitrocellulose filters. The filters were incubated with primary antibodies and then with peroxidase-conjugated immunoglobulin G antibodies (MBL). The immune complex was visualized by CSA ECL system (Amersham). Antibodies for mTOR, PKM1 (Epitomics), TLR4, PKM2 (Abnova), phosphorylated mTOR (pSer2448; Assay Biotechnology), RAGE, beclin-1 (Santa Cruz Biotechnology), LC3 (CosmoBio), BCL-2 (DAKO), and tubulin (loading control; Oncogene Research) were used as primary antibodies. For immunoprecipitation, the blots were incubated first with primary antibodies for beclin-1 (Santa Cruz) or BCL-2 (DAKO).

Reverse transcriptase PCR

RAGE mRNA was detected by reverse transcriptase PCR using total RNA (0.5 μg) extracted with RNeasy kit (Qiagen). The

Published OnlineFirst November 6, 2013; DOI: 10.1158/0008-5472.CAN-13-1052

primer sets used to amplify rat HMGB1 (GenBank accession no. NM_012963.20) were forward 5′-GAGCACAAGAAGAAG-CACCC-3′ and reverse 5′-TAACGAGCCTTGTCAGCCTT-3′ (synthesized by Sigma Genosys).

ELISA

Assay kits were used to measure concentrations of HMGB1 (Shino-test), glutamine (MyBioSource), 1,3-bisphosphoglycerate (Uscn Life Science), pyruvate (JK International), PK (Cusabio Biotech), acetyl-CoA (AcCoA; Abnova), lactate, α-ketoglutarate (Biovision), malate (Abcam), and interleukin (IL)-1β (Uscan), and IL-6 (ENZO Life Science). MitoTracker green (MTG; Invitrogen) was used to measure mitochondrial volume and membrane potential (MV; ENZO) according to the manufacturer's instructions.

Measurement of ^{13}C-labeled metabolites by LC-MS

Thin slices of muscle were placed in 3.5-cm dishes and cultured in regular medium supplemented with 2 mmol/L ^{13}C-glutamine (Isotech) for 12 hours. Fresh medium was simultaneously incubated without cells as a reference. Cells were then lysed with a solution of 50% methanol/30% acetonitrile in water stored in dry ice/methanol, and then quickly scraped. The lysate was centrifuged at 16,000 × *g* for 15 minutes at 0°C, and the supernatant was collected for liquid chromatography/mass spectrometry (LC/MS) analysis. The 18,000 cells were lysed in 1 mL of extraction solution. Intermediates were separated using a liquid chromatography system.

siRNA and microRNA

FlexiTube siRNAs for RAGE and TLR4, and AllStars Negative Control siRNA were purchased from Qiagen Genomics. Cells were transfected with 50 nmol/L siRNA using Lipofectamine 2000 (Invitrogen), according to the manufacturer's instructions. For administration of GLS glutaminase miTarget miRNA (GeneCopoeia), 100 pmol of miRNA was encapsulated in 2 mL of cationic liposome (EL-C-01, DPPC: 26 mmol/L, Nippon Oil&Fats), and 200 μL of the solution was administered intraperitoneally twice a week (28, 29).

Statistical analysis

Statistical significance was examined by ANOVA, a two-tailed, unpaired Mann–Whitney test, and a Spearman test using InStat software (GraphPad). Statistical significance was defined as a two-sided $P < 0.05$. Cluster analysis was performed by the Ward method.

Results

Serum concentration of HMGB1 in patients with colorectal cancer

HMGB1 expression has been shown to be closely associated with colorectal cancer progression (15, 18, 30). In the present study, serum HMGB1 concentration was examined in 10 healthy volunteers and 46 patients with colorectal cancer. As shown in Table 1, HMGB1 concentration was significantly associated with colorectal cancer stage ($P < 0.0001$).

Table 1. Concentration of serum HMGB1 and glutamine in patients with colorectal cancer

Stage[a]	*n*	Serum HMGB1 concentration (ng/mL)	Serum glutamine concentration (μmol/L)
Control	10	32.4 ± 15.4	512.3 ± 49.5
I	16	91.8 ± 48.2	520.8 ± 51.9
II	13	236.4 ± 134.4	543.5 ± 55.2
III	11	518.4 ± 193.4	577.1 ± 53.8
IV	6	751.3 ± 196.0	612.7 ± 61.4

[a]Pathology stage was classified according to the TNM classification (46). Stage I, tumor within the mucosae propria or submucosal layers; stage II, tumor invades beyond the muscularis propria without lymph node metastasis; stage III, tumor shows lymph node metastasis; stage IV, lymph node metastases may or may not be observed, distant metastases may be observed.

Effect of HMGB1 on muscle tissues

The effect of HMGB1 on normal tissues was examined in an *ex vivo* mouse soleus muscle model (Fig. 1). Expression of the HMGB1 receptors TLR4 and RAGE in muscle tissue and colorectal cancer cells was confirmed by Western blotting (Fig. 1A). PK mediates the linker reaction between glycolysis and the TCA cycle, which is followed by oxidative phosphorylation. PKM1 is expressed in mature tissues, whereas PKM2 is expressed in embryonic tissues and cancer cells. In CT26 and HT29 colorectal cancer cells, PKM2 expression was higher than PKM1 expression. After HMGB1 treatment, PKM1 levels in colorectal cancer cells decreased; however, PKM2 levels were not altered (Fig. 1B). HMGB1 treatment decreased PKM1 production, which was only produced in the muscle. Knockdown of RAGE abrogated the HMGB1-induced PKM1 decrease in colorectal cancer cells and muscle (Fig. 1C). In contrast, knockdown of TLR4 did not affect the HMGB1-induced PKM1 decrease. Following HMGB1 treatment, PK activity decreased in the muscle but not in colorectal cancer cells (Fig. 1D).

Mitochondrial function of HMGB1-treated tissues

A decrease in the reaction that produces pyruvate could suppress oxidative energy production. In the *ex vivo* analysis, HMGB1 did not affect mitochondrial density or membrane voltage in the muscle (Fig. 1E and F). The ATP concentration in colorectal cancer cells was not altered by HMGB1. In contrast, following HMGB1 treatment, the ATP level in the muscle decreased by 17% (Fig. 1G). The lactate concentration increased in colorectal cancer cells, whereas in the muscle, lactate was not altered and remained at low levels (Fig. 1H).

Effect of HMGB1 on the amino acid profiles in mice

The effect of HMGB1 on normal mouse tissues was examined. Male BALB/c mice were administered HMGB1 (4.5 mg/kg

Published OnlineFirst November 6, 2013; DOI: 10.1158/0008-5472.CAN-13-1052

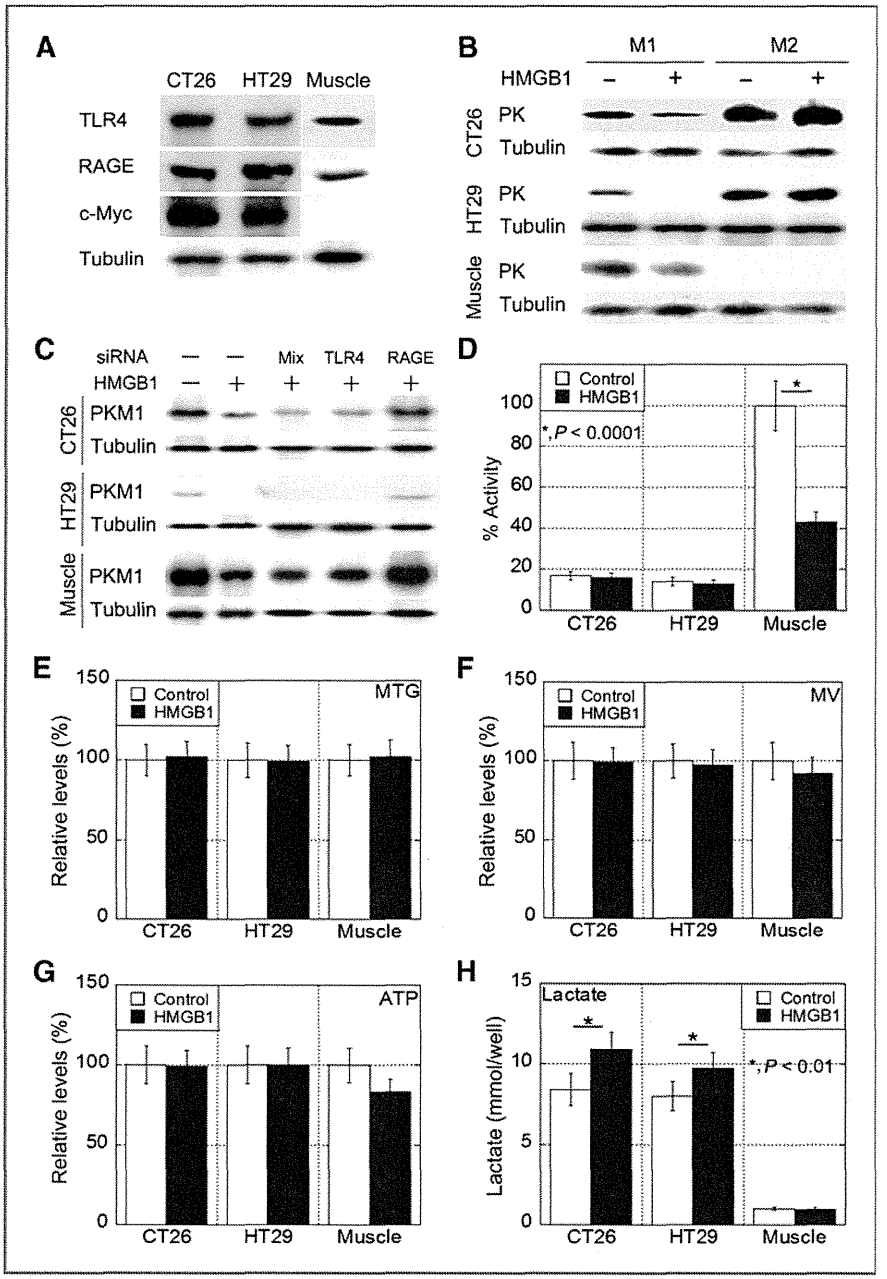

Figure 1. Effect of HMGB1 on energy production in colorectal cancer cells and mouse muscle. A, protein expression of TLR4, RAGE, and c-Myc in CT26 and HT29 colorectal cancer cells and mouse soleus muscle, which was treated by an *ex vivo* method. B and D, protein expression of PKM1 (M1) and PKM2 (M2; B) and PK activity (D) in untreated and HMGB1-treated colorectal cancer cells and mouse muscle. C, effect of RAGE and TLR4 knockdown on PKM1 production in colorectal cancer cells and mouse muscle following HMGB1 treatment. E–H, mitochondrial content as measured by MTG staining (E), mitochondrial membrane voltage (F), ATP levels (G), and lactate (H) in colorectal cancer cells and mouse muscle. Bar, SD.

body weight) by intraperitoneal injection (Fig. 2A). Physical abnormalities and inhibition of body weight gain were not observed in HMGB1-treated mice. However, HMGB1 treatment decreased PKM1 production and PK activity in the muscle (Fig. 2B and C). HMGB1 treatment also affected the PFAA profile, and glutamate levels increased (Fig. 2C). In the soleus muscle, the levels of all amino acids except aspartate decreased. At autopsy, the serum concentrations of IL-1β and IL-6 were also measured (Fig. 2D). HMGB1-treated mice had higher levels of IL-1β and IL-6 than PBS-injected mice.

Induction of autophagy in mouse muscle by HMGB1

We examined the mechanism underlying HMGB1-associated autophagy induction using an *ex vivo* assay of mouse muscle (Fig. 2E to H). HMGB1 treatment reduced mTOR phosphorylation, which induced autophagy-related beclin-1 and LC3bII expression in the muscle (Fig. 2E). HMGB1 treatment also induced p38 phosphorylation, which is required for activation of the autophagy machinery (Fig. 2F). Treatment with a p38 inhibitor inhibited LC3 upregulation. Knockdown of the HMGB1 receptor RAGE reduced the dephosphorylation of

Published OnlineFirst November 6, 2013; DOI: 10.1158/0008-5472.CAN-13-1052

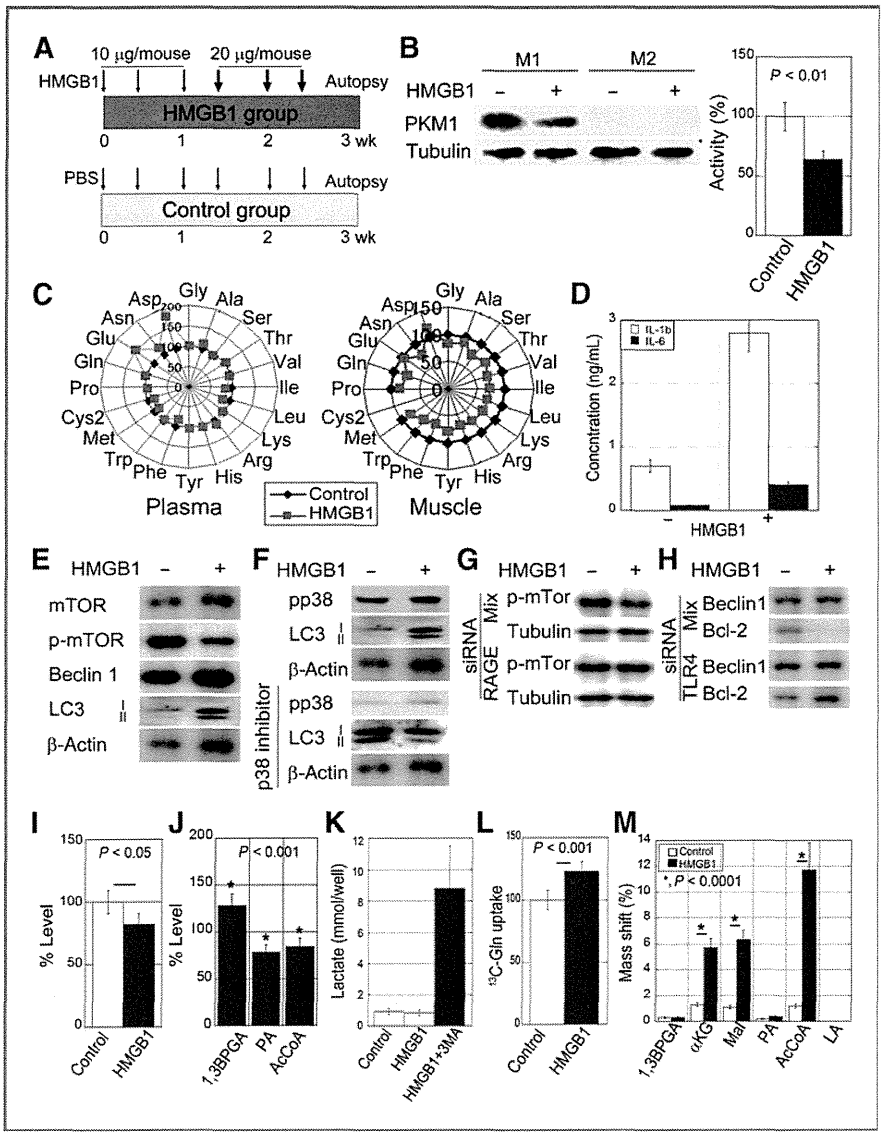

Figure 2. Effect of HMGB1 on the plasma amino acid profile and metabolism in mouse muscle. A, protocol for HMGB1 injection into male BALB/c mice. B, protein expression of PKM1 (M1) and PKM2 (M2), and PK activity in the soleus muscles of untreated and HMGB1-treated mice. C, amino acid concentration in the plasma and muscle of untreated and HMGB1-treated mice. Bar, SE. D, serum concentrations of IL-1β and IL-6 in HMGB1-treated mice. E, effect of HMGB1 on the protein expression of mTOR, phosphorylated mTOR (p-mTOR), beclin-1, and LC3. F, effect of HMGB1 on p38 phosphorylation and LC3 expression; a p38 inhibitor (SB239063) was used. G, effect of RAGE knockdown on mTOR phosphorylation. H, effect of RAGE knockdown on beclin-1 expression. The precipitates were probed with an anti-Beclin1 or anti-Bcl-2 antibody. I, protein content. J, levels of 1,3-bisphosphoglycerate (1,3BPG), pyruvate (PA), and AcCoA were examined by ELISA. K, effect of inhibiting autophagy by 3MA on lactate levels. L, uptake of ^{13}C-labeled glutamine in the lysate was examined by mass analysis. M, integration of ^{13}C into 1,3BPG, α-KG, malate (Mal), pyruvate, AcCoA, and lactate (LA) in muscle tissue. Bar, SD.

mTOR (Fig. 2G). Therefore, mTOR inactivation occurred in response to RAGE activation by HMGB1. In contrast, knockdown of another HMGB1 receptor, TLR4, abrogated the coprecipitation of Bcl-2 with beclin-1 (Fig. 2H). Therefore, HMGB1 activated beclin-1 through TLR4 signaling. HMGB1 treatment decreased the total protein levels in the muscle (Fig. 2I). Because PK links glycolysis to the TCA cycle by supplying AcCoA, the levels of an upstream member of the PK pathway (1,3-bisphosphoglycerate; 1,3BPGA), a downstream product of PK (pyruvate), and AcCoA were examined (Fig. 2J). Treatment of the muscle with HMGB1 increased 1,3BPGA levels and decreased pyruvate and AcCoA levels. Treatment with 3MA inhibited autophagy and significantly increased lactate levels (Fig. 2K). HMGB1 increased glutamine uptake in the muscle (Fig. 2L). The ^{13}C-labeled glutamine was markedly increased in the muscle and was incorporated into α-ketoglutamate (α-KG), malate, and AcCoA, but not into lactate (Fig. 2M).

Alteration of the PFAA profile in mouse colon carcinogenesis

PFAA profiles were during the development of colon cancer using a DMH-induced C57BL/6 mouse colon cancer model. The PFAA profiles were examined at 25, 35, and 40 weeks after starting DMH administration (Fig. 3A). Adenoma and carcinoma were not observed at week 25, whereas carcinoma was observed in all mice at week 40 (Fig. 3B). In the DMH-induced mouse colon cancer model, HMGB1 was increased, during the colonic carcinogenic process (Fig. 3C to E). Plasma HMGB1 protein levels and mucosal HMGB1 mRNA and protein levels were temporally increased. As

Published OnlineFirst November 6, 2013; DOI: 10.1158/0008-5472.CAN-13-1052

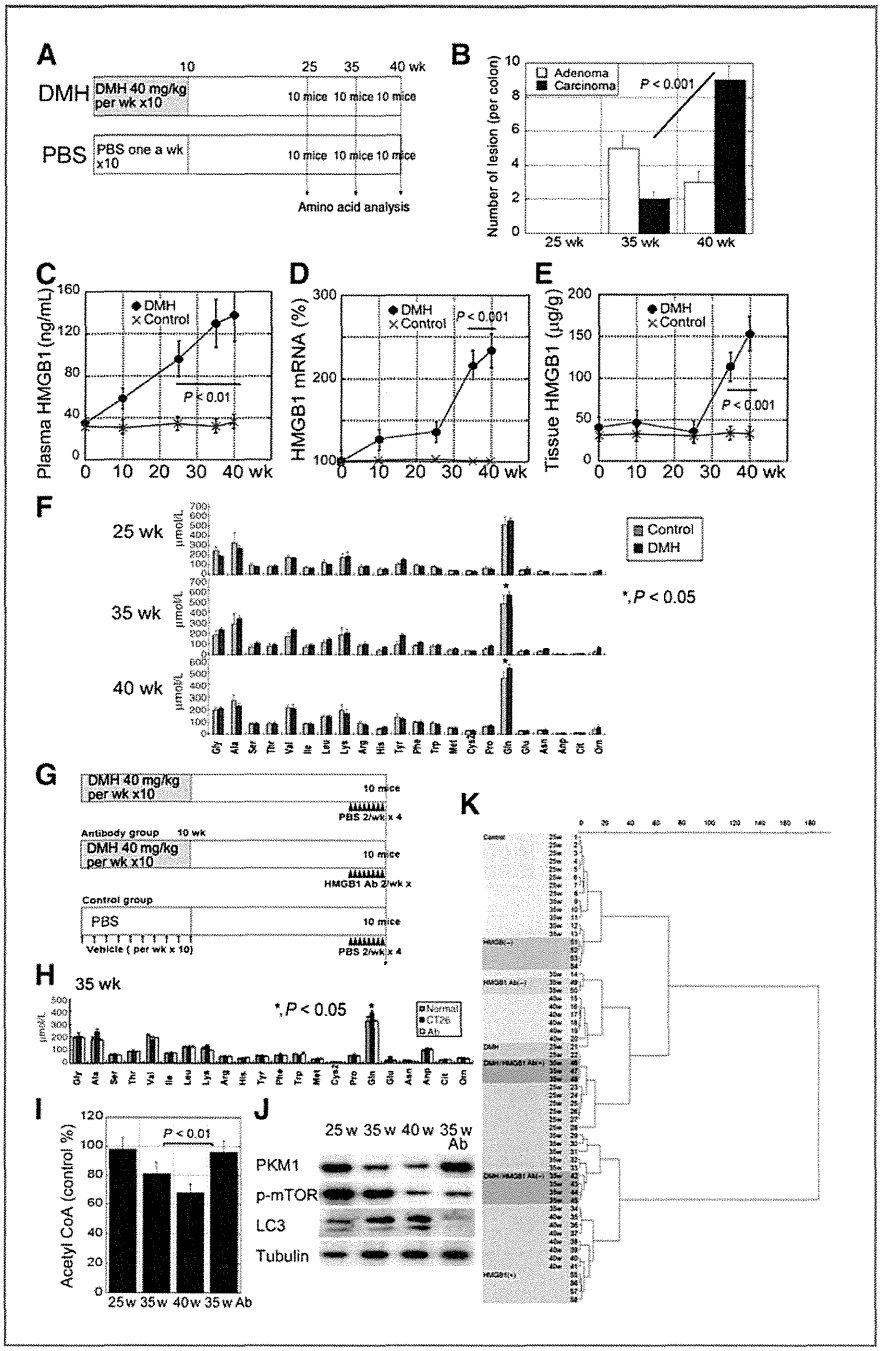

Figure 3. Effect of HMGB1 on the plasma amino acid profile in a mouse colon cancer model. A, protocol for the DMH-induced colon cancer model using male C57BL/6 mice. B, occurrence of colon neoplasms. C–E, plasma HMGB1 protein (C), mucosal *HMGB1* mRNA (D), and mucosal HMGB1 protein (E) levels in DMH-injected C57BL/6 mice. F, amino acid concentrations in the plasma at 25, 35, and 40 weeks were compared with those in the PBS-injected control mice. Bar, SE. G, protocol for the DMH-induced colon cancer model using male C57BL/6 mice treated with an anti-HMGB1 antibody. H, amino acid concentrations in the plasma at week 35 were compared with those in the anti-HMGB1 antibody-injected mice. Bar, SE. I–J, the levels of AcCoA (I) and protein levels of PKM1, phosphorylated mTOR (p-mTOR), and LC3 (J) in the muscle of DMH-injected mice at weeks 25, 35, and 40. 35w Ab: DMH-injected mice treated with an anti-HMGB1 antibody. K, cluster analysis of the PFAA profiles in the DMH-induced carcinogenesis model (Fig. 3) and HMGB1-treated mice (Fig. 1) using the Ward method.

shown in Fig. 3F, the levels of several plasma amino acids were altered. In particular, glutamine levels increased in DMH-treated mice. To examine the role of HMGB1 on the PFAA profile in DMH-treated mice, HMGB1 activity was inhibited with a neutralizing anti-HMGB1 antibody (Fig. 3G). The PFAA profiles in groups of PBS injection, DMH treatment, and DMH treatment with anti-HMGB1 antibody were compared (Fig. 3H). The PFAA profile of the anti-HMGB1 antibody-administered DMH-treated mice with was the same as that of the control mice, but differed from the profile of the DMH-treated mice. In the soleus muscle, AcCoA and PKM1 were lower, whereas p-mTOR and LC3 were higher at weeks 35 and 40 than at week 25 (Fig. 3I and J). Cluster analysis showed that the PFAA profiles of DMH-model mice

Published OnlineFirst November 6, 2013; DOI: 10.1158/0008-5472.CAN-13-1052

(week 25), DMH-untreated mice, anti-HMGB1 antibody-treated DMH-model mice, and PBS-injected mice belonged to the same cluster. In contrast, DMH-model mice (weeks 35 and 40), control serum-treated DMH-model mice, and HMGB1-injected mice belonged to the other cluster (Fig. 3K and Supplementary Table S1). These findings suggest that the HMGB1 concentration is the most relevant factor distinguishing the different clusters based on PFAA profile. To confirm the importance of HMGB1 on free amino acid metabolism, the serum concentrations of HMGB1 and glutamine were compared (Table 1). The concentrations of HMGB1 and glutamine were significantly correlated (Spearman $r = 0.9824$, $P < 0.01$). The concentration of glutamine was also associated with cancer stage ($P < 0.01$).

Alteration of muscle metabolism in mice with subcutaneous cancer

Plasma HMGB1 levels and metabolism in the muscle were examined in CT26 tumor-burdened BALB/c mice and HT29 tumor-burdened nude mice (Fig. 4). At 4 weeks, the tumors were growing and HMGB1 levels were increased (Fig. 4A). After 4 weeks, the muscle tissues showed decreased PKM1 expression and PK activity; however, no induction of PKM2 was observed (Fig. 4B and C). The ATP levels and mitochondrial voltages did not differ from those in control mice (Fig. 4D). Levels of 1,3BPGA increased, whereas pyruvate and AcCoA decreased (Fig. 4E). The glutamine carbons administered before sacrifice were mainly integrated into AcCoA (Fig. 4F).

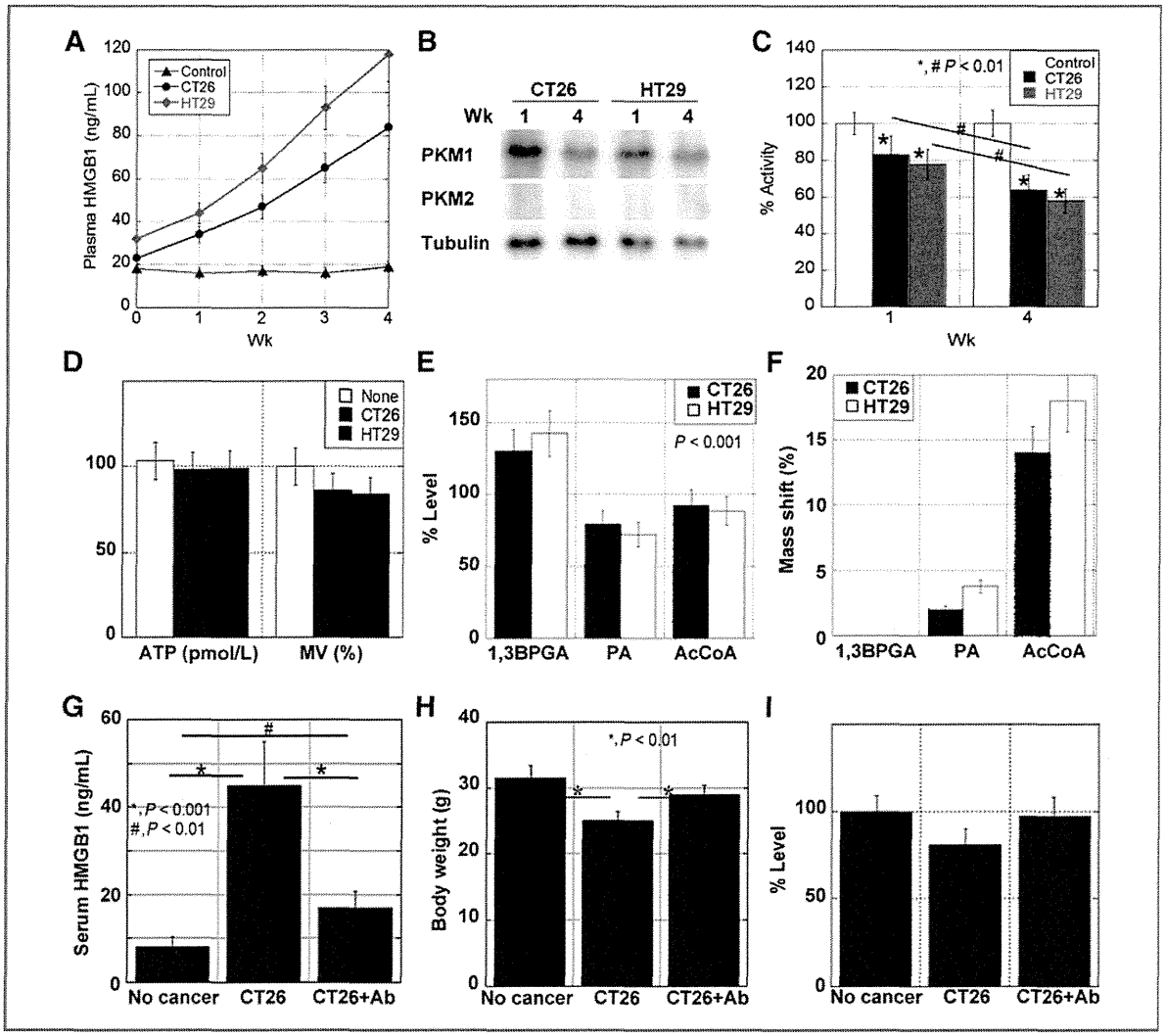

Figure 4. Examination of the soleus muscles of mice burdened with subcutaneous CT26 or HT29 tumors. A, temporal alteration of plasma HMGB1. B and C, protein levels of PKM1 and PKM2 (B), and PK activity (C) at weeks 1 and 4. D, the levels of ATP and mitochondrial membrane voltage (MV) at week 4. E, levels of 1,3BPGA, pyruvate (PA), and AcCoA at week 4. F, integration of ^{13}C into 1,3BPGA; pyruvate; and AcCoA at week 4. G–I, effect of anti-HMGB1 antibody (30 μg, i.p., twice a week) on serum HMGB1 (G), body weight (H), and protein content in the muscle (I). Bar, SD.

Published OnlineFirst November 6, 2013; DOI: 10.1158/0008-5472.CAN-13-1052

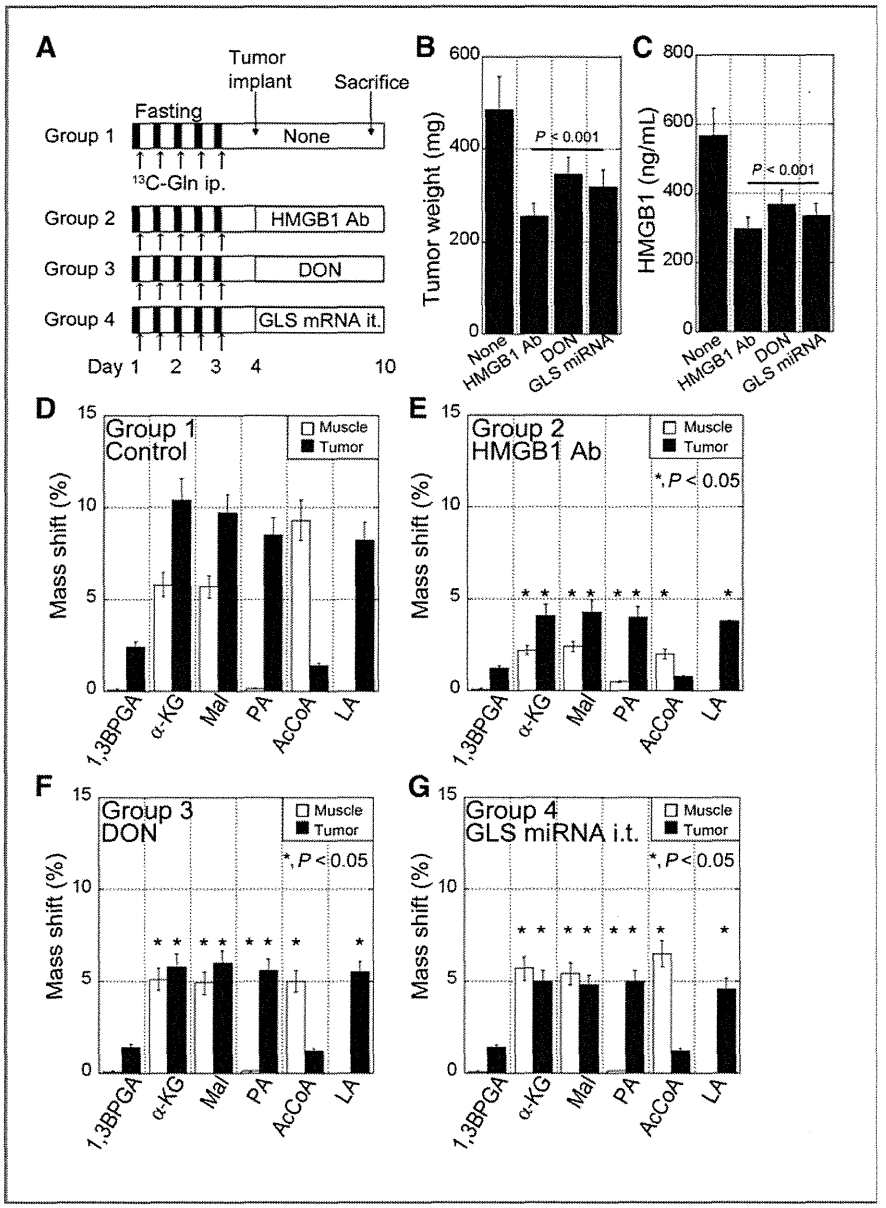

Figure 5. Transfer of glutamine from muscle to tumor. A, protocol for the animal model. ^{13}C-Gln was integrated into BALB/c mouse tissues using repeated fasting cycles (4-hour fasting, 8-hour feeding). After five cycles, a CT26 tumor (5 × 5 × 5 mm^3), which was grown subcutaneously in another mouse, was implanted into the ^{13}C-Gln-administrated mice. After implantation, the mice were treated with PBS intraperitoneally (group 1), an anti-HMGB1 antibody intraperitoneally (group 2), DON intraperitoneally (group 3), or GLS siRNA intratumoral injection (group 4). B and C, tumor weight and serum HMGB1 levels in each group. D–G, integration of ^{13}C into 1,3BPGA, α-ketoglutarate (α-KG, malate (Mal), pyruvate (PA), AcCoA, and lactate (LA) in the tumor tissues in the four groups. Bar, SD. E–G, *, statistically significant difference versus group 1.

In the CT26 subcutaneous tumor model, a neutralizing anti-HMGB1 antibody was administered intraperitoneally to inactivate HMGB1 (Fig. 4G to I). The antibody treatment decreased the serum HMGB1 concentration secreted by CT26 tumors, which induced gains in both body weight and the protein content of mouse tissues.

Utilization of muscle glutamine by cancer cells

Finally, we aimed to elucidate the muscle-tumor glutamine cycle in a mouse tumor model (Fig. 5). A fasting-feeding cycle was repeated five times with ^{13}C-glutamine injection to increase uptake of ^{13}C-glutamine into the muscles of BALB/c mice (Fig. 5A; ref. 24). Then the mice were inoculated subcutaneously with CT26 tumors and were treated with an inhibitory agent of the glutamine cycle, an anti-HMGB1 antibody, an inactive glutamine analog, DON, and knockdown of glutaminase (GLS). Inhibition of the glutamine cycle decreased tumor growth and HMGB1 production from the tumors (Fig. 5B and C). As shown in Fig. 5D to G, the intratumoral distribution of ^{13}C-glutamine from the muscle was examined. In control mice, HMGB1 secreted from cancer cells increased ^{13}C-glutamine integration into AcCoA, and the muscle ^{13}C-glutamine was transferred to cancer cells, which was mainly integrated into lactate (Fig. 5D). In contrast, treatment with the neutralizing

Published OnlineFirst November 6, 2013; DOI: 10.1158/0008-5472.CAN-13-1052

anti-HMGB1 antibody decreased ^{13}C-glutamine integration into α-ketoglutarate, malate, and pyruvate in the cancer cells and muscle. In particular, it decreased ^{13}C-glutamine integration into lactate in the cancer cells and into AcCoA in the muscle (Fig. 5E). Treatment with the inactive glutamine analog DON had an effect similar to that in the anti-HMGB1 antibody-treated mice (Fig. 5F). The effect of GLS microRNA injection into the tumor on the tumor ^{13}C-glutamine integration pattern was similar to that in the DON-treated mice (Fig. 5G). Interestingly, the ^{13}C-glutamine integration in the muscle was also similar to that in the DON-treated mice, which might be due to the reduced HMGB1 levels.

Discussion

In the present study, we examined the effects of HMGB1 on PK status and autophagy-proteolysis in muscle. HMGB1 decreased production of the PKM1 isoform in the muscles, which did not produce PKM2. In contrast, treatment of CT26 and HT29 colorectal cancer cells, which produce both PKM1 and PKM2, with HMGB1 decreased only PKM1. It has been shown that c-Myc is responsible for switching the expression from *PKM1* to *PKM2* (4); however, c-Myc is not expressed in the muscle. Therefore, PKM1-PKM2 switching did not occur, and PK activity decreased. This PK inactivation decreased the supply of pyruvate and AcCoA (downstream of pyruvate); however, mitochondrial energy production was maintained without increasing lactate production. To compensate for the decreased production of AcCoA from pyruvate, glutamine was used to supply α-ketoglutarate to the TCA cycle. The results of the carbon chase experiments indicated that glutamine was metabolized to produce primarily AcCoA so that the TCA cycle could continue to produce energy. We also examined the effect of HMGB1 on the liver (data not sown). The liver expresses the liver form of PK (PKLR) instead of PKM1 and PKM2. Because PKLR was not affected by HMGB1, the liver maintained aerobic energy production without glutamine usage. These results suggest that HMGB1-affected muscle might utilize amino acids as substrates for the TCA cycle.

To use amino acids as an energy source, free amino acids need to be generated from proteins. Our data suggest that in the presence of HMGB1, proteolysis associated with autophagy was induced. Autophagy involves the selective degradation of cellular components, including aged proteins, protein debris, and damaged organelles, which results in nutrient recycling and energy generation (10, 31). Autophagy is coupled with ubiquitination and subsequent proteasomal degradation in the protein quality control system (9, 32). Therefore, we examined autophagy signals in the tissues of HMGB1-treated mice. HMGB1 induced the dephosphorylation of mTOR, which upregulated the autophagy-associated proteins beclin-1 and LC3II through RAGE-associated p38 phosphorylation. RAGE has been shown to induce sustained autophagy and suppress apoptosis (33).

Moreover, HMGB1 activates TLR4 to release beclin-1 from the complex with Bcl-2. TLR4-induced autophagy is associated with defense against microbes, inflammation, and tumorigenesis (21, 22). Therefore, HMGB1 induces proteolysis through autophagy, which might supply free amino acids. An autophagy-induced glutamine supply might be important for maintaining mitochondrial energy production in the muscle. Bluemlein and colleagues stated that PK maintains amino acid homeostasis, whereas low PK increases cellular glutamine (34).

AcCoA generation from glutamine is thought to be an adaptation for retaining aerobic energy production in cancer-burdened hosts. Indeed, inhibition of autophagy by 3MA decreased AcCoA levels and induced lactate production in the muscle.

In contrast, cancer cells utilize glucose and glutamine as a carbon skeleton and produce energy through lactate fermentation (35, 36). HMGB1 treatment increased lactate fermentation in colorectal cancer cells in culture. Moreover, cancer cells consumed the plasma glutamine released from the muscle. The mouse model of muscle-integrated ^{13}C-glutamine showed that it was used for lactate fermentation in the cancer cells. These findings suggest a cancer–host relationship in energy production. DeBerardinis and Cheng have advocated a cancer–muscle relationship through glutamine (37). They showed that glutamine is utilized to deliver carbon to the TCA cycle in cancer cells. c-Myc activation switches mitochondrial metabolism from glucose dependent to glutamine dependent (38, 39). The glutamine dependency of cancer cells is diverse. However, the possibility of this cancer–muscle relationship should be considered when treating patients with cancer (40). The wasting of muscle protein due to cancer–muscle interaction is an important mechanism that causes cachexia (37). Some "aberrant" energy production systems have been reported in cancer cells. For adapting hypoxic-hypoglucemic condition, some cancer uses fumarate as an energy source, which is known to occur in parasites (41).

In our experiments, the PFAA profile was altered because of autophagy, proteolysis, and utilization of amino acid as an energy source. From the present study and our previous reports, HMGB1 levels were increased beginning in the early stage of colon carcinogenesis (20). The PFAA profile was also altered during DMH-induced colon cancer development, and this alteration, including the increased glutamine, occurred before and after the neoplasm developed. These alterations in the PFAA profile resulted from the effects of HMGB1 on catabolism and energy production in the muscle, which altered amino acid metabolism. Cluster analysis clearly showed that the PFAA profiles were primarily distinguished by the level of HMGB1 (Fig. 3K). In addition to the mouse model results, human data for HMGB1 and glutamine showed evidence for this relationship at every stage of human colorectal cancer. Therefore, the PFAA profile might reflect a carcinogenic change, and could provide an opportunity to detect carcinogenic processes at the preclinical and precancerous phases (12). The PFAA profile in patients with several human cancers has been reported to be altered from that in healthy volunteers (12, 42). These findings suggest that the PFAA profile might be a sensitive probe of altered host metabolism due to cancer development.

Cancer possesses a chronic inflammation aspect, which could also alter the amino acid metabolism of the host. HMGB1

Published OnlineFirst November 6, 2013; DOI: 10.1158/0008-5472.CAN-13-1052

is a key factor in innate immunity as a ligand of TLR4. The HMGB1-injected mouse model (Fig. 2) showed increased serum IL-1β and IL-6. These inflammatory cytokines are also candidates for catabolic factors in patients with cancer (43). Excessively high concentrations of HMGB1 induce apoptosis of macrophages and macrophage-lineage dendritic cells (15), and modest levels of HMGB1 induce inflammatory cytokines and might concurrently alter muscle metabolism. In the present study, neutralization of HMGB1 abrogated the changes in the PFAA profile in the carcinogenesis model. Therefore, HMGB1 might alter muscle metabolism both directly and through inflammatory cytokines.

Cancer cells consume both glucose and glutamine as energy sources, targeting just one of them, glutamine, is sufficient to suppress cancer growth, because glutamine is essential in DNA synthesis (24). Glutamine targeting using the inactive analog DON or GLS knockdown has been reported to be effective in suppressing cancer metastasis in an animal model (25). Our data also showed that glutamine targeting with an anti-HMGB1 antibody, DON, or GLS knockdown inhibited the growth of subcutaneous tumors. Inhibition of tumor growth decreased HMGB1 secretion, which abrogated the cancer–muscle relationship. Despite the difference in the PFAA of human and mouse, patients with colorectal cancer also show increased plasma glutamine (12). This suggests that glutamine targeting should be attempted in human patients with colorectal cancer.

Glutamine targeting is a way to correct the abnormal PFAA profile. For example, autophagy-induced malnutrition leads to compromised immunity and cancer progression; thus, tolerance to anticancer treatment might be diminished (44). To avoid extreme catabolic changes in cancer-burdened hosts with altered energy production, an adequate amino acid supply could be important. The necessity of supplying branched side chain amino acids to cancer-burdened hosts has been proposed (44). The observed PFAA profile suggests altered energy production in the host. A suitable amino acid supply could be necessary to improve energy production in a case-specific manner. This concept might be applicable to other diseases in addition to cancer.

HMGB1 is released in bulk from necrotic cancer cells, and activates living cancer cells to regrow (45). Adding these findings to the present observations, HMGB1 released from necrotic cancer cells might induce the degradation of host muscle tissues by autophagy to provide glutamine to the remnant cancer cells. Particularly in this situation, targeting HMGB1 and/or glutamine should be emphasized.

Disclosure of Potential Conflicts of Interest

No potential conflicts of interest were disclosed.

Authors' Contributions

Conception and design: H. Kuniyasu
Development of methodology: T. Sasaki
Acquisition of data (provided animals, acquired and managed patients, provided facilities, etc.): Y. Luo, J. Yoneda, K. Shimbo, S. Eto, Y. Kato, H. Miyano, T. Kobayashi
Analysis and interpretation of data (e.g., statistical analysis, biostatistics, computational analysis): Y. Luo, J. Yoneda, T. Sasahira, Y. Chihara, H. Kuniyasu
Writing, review, and/or revision of the manuscript: Y. Luo, H. Kuniyasu
Administrative, technical, or material support (i.e., reporting or organizing data, constructing databases): T. Sasaki, T. Sasahira
Study supervision: H. Kuniyasu

Acknowledgments

The authors thank Tomomi Masutani and Kayo Fukunishi for expert assistance with the preparation of this article.

Grant Support

This work was supported in part by Grant-in-Aid for Scientific Research from Japan Society for the Promotion of Science (23659188, 23590430, and 24590450).

The costs of publication of this article were defrayed in part by the payment of page charges. This article must therefore be hereby marked *advertisement* in accordance with 18 U.S.C. Section 1734 solely to indicate this fact.

Received April 15, 2013; revised September 6, 2013; accepted September 29, 2013; published OnlineFirst November 6, 2013.

References

1. Warburg O. On respiratory impairment in cancer cells. Science 1956;124:269–70.
2. Koppenol WH, Bounds PL, Dang CV. Otto Warburg's contributions to current concepts of cancer metabolism. Nat Rev Cancer 2011;11:325–37.
3. Mazurek S. Pyruvate kinase type M2: a key regulator of the metabolic budget system in tumor cells. Int J Biochem Cell Biol 2011;43:969–80.
4. David CJ, Chen M, Assanah M, Canoll P, Manley JL. HnRNP proteins controlled by c-Myc deregulate pyruvate kinase mRNA splicing in cancer. Nature 2010;463:364–8.
5. Christofk HR, Vander Heiden MG, Wu N, Asara JM, Cantley LC. Pyruvate kinase M2 is a phosphotyrosine-binding protein. Nature 2008;452:181–6.
6. Hitosugi T, Kang S, Vander Heiden MG, Chung TW, Elf S, Lythgoe K, et al. Tyrosine phosphorylation inhibits PKM2 to promote the Warburg effect and tumor growth. Sci Signal 2009;2:ra73.
7. Morifuji M, Ishizaka M, Baba S, Fukuda K, Matsumoto H, Koga J, et al. Comparison of different sources and degrees of hydrolysis of dietary protein: effect on plasma amino acids, dipeptides, and insulin responses in human subjects. J Agric Food Chem 2010;58:8788–97.
8. Hammer JA III, Rannels DE. Protein turnover in pulmonary macrophages. Utilization of amino acids derived from protein degradation. Biochem J 1981;198:53–65.
9. Kadowaki M, Kanazawa T. Amino acids as regulators of proteolysis. J Nutr 2003;133:2052S–6S.
10. Jung CH, Ro SH, Cao J, Otto NM, Kim DH. mTOR regulation of autophagy. FEBS Lett 2010;584:1287–95.
11. Kamaura M, Nishijima K, Takahashi M, Ando T, Mizushima S, Tochikubo O. Lifestyle modification in metabolic syndrome and associated changes in plasma amino acid profiles. Circ J 2010;74:2434–40.
12. Miyagi Y, Higashiyama M, Gochi A, Akaike M, Ishikawa T, Miura T, et al. Plasma free amino acid profiling of five types of cancer patients and its application for early detection. PLoS One 2011;6:e24143.
13. Okamoto T, Yamagishi S, Inagaki Y, Amano S, Koga K, Abe R, et al. Angiogenesis induced by advanced glycation end products and its prevention by cerivastatin. FASEB J 2002;16:1928–30.
14. Taguchi A, Blood DC, del Toro G, Canet A, Lee DC, Qu W, et al. Blockade of RAGE-amphoterin signalling suppresses tumour growth and metastases. Nature 2000;405:354–60.
15. Ohmori H, Luo Y, Kuniyasu H. Non-histone nuclear factor HMGB1 as a therapeutic target in colorectal cancer. Expert Opin Ther Targets 2011;15:183–93.

Published OnlineFirst November 6, 2013; DOI: 10.1158/0008-5472.CAN-13-1052

16. Scaffidi P, Misteli T, Bianchi ME. Release of chromatin protein HMGB1 by necrotic cells triggers inflammation. Nature 2002;418:191–5.
17. Gardella S, Andrei C, Ferrera D, Lotti LV, Torrisi MR, Bianchi ME, et al. The nuclear protein HMGB1 is secreted by monocytes via a non-classical, vesicle-mediated secretory pathway. EMBO Rep 2002;3: 995–1001.
18. Kuniyasu H, Chihara Y, Takahashi T. Co-expression of receptor for advanced glycation end products and the ligand amphoterin associates closely with metastasis of colorectal cancer. Oncol Rep 2003; 10:445–8.
19. Kuniyasu H, Chihara Y, Kondo H. Differential effects between amphoterin and advanced glycation end products on colon cancer cells. Int J Cancer 2003;104:722–7.
20. Ohmori H, Luo Y, Fujii K, Sasahira T, Shimomoto T, Denda A, et al. Dietary linoleic acid and glucose enhances azoxymethane-induced colon cancer and the metastasis through the expression of high mobility group box 1. Pathobiology 2010;77:210–7.
21. Ioannou S, Voulgarelis M. Toll-like receptors, tissue injury, and tumourigenesis. Mediators Inflamm 2010;2010.pii: 581837.
22. Delgado MA, Deretic V. Toll-like receptors in control of immunological autophagy. Cell Death Differ 2009;16:976–83.
23. Tang D, Kang R, Livesey KM, Cheh CW, Farkas A, Loughran P, et al. Endogenous HMGB1 regulates autophagy. J Cell Biol 2010;190: 881–92.
24. Wagenmakers AJ. Muscle amino acid metabolism at rest and during exercise: role in human physiology and metabolism. Exerc Sport Sci Rev 1998;26:287–314.
25. Shelton LM, Huysentruyt LC, Seyfried TN. Glutamine targeting inhibits systemic metastasis in the VM-M3 murine tumor model. Int J Cancer 2010;127:2478–85.
26. Shimbo K, Oonuki T, Yahashi A, Hirayama K, Miyano H. Precolumn derivatization reagents for high-speed analysis of amines and amino acids in biological fluid using liquid chromatography/electrospray ionization tandem mass spectrometry. Rapid Commun Mass Spectrom 2009;23:1483–92.
27. Kuniyasu H, Oue N, Wakikawa A, Shigeishi H, Matsutani N, Kuraoka K, et al. Expression of receptors for advanced glycation end-products (RAGE) is closely associated with the invasive and metastatic activity of gastric cancer. J Pathol 2002;196:163–70.
28. Chihara Y, Fujimoto K, Kondo H, Moriwaka Y, Sasahira T, Hirao Y, et al. Anti-tumor effects of liposome-encapsulated titanium dioxide in nude mice. Pathobiology 2007;74:353–8.
29. Kuniyasu H, Oue N, Sasahira T, Luo Y, Moriwaka Y, Shimomoto T, et al. Reg IV enhances peritoneal metastasis in gastric carcinomas. Cell Prolif 2009;42:110–21.
30. Lee H, Song M, Shin N, Shin CH, Min BS, Kim HS, et al. Diagnostic significance of serum HMGB1 in colorectal carcinomas. PLoS ONE 2012;7:e34318.
31. Levine B, Klionsky DJ. Development by self-digestion: molecular mechanisms and biological functions of autophagy. Dev Cell 2004; 6:463–77.
32. Su H, Wang X. p62 Stages an interplay between the ubiquitin-proteasome system and autophagy in the heart of defense against proteotoxic stress. Trends Cardiovasc Med 2011;21:224–8.
33. Kang R, Tang D, Schapiro NE, Livesey KM, Farkas A, Loughran P, et al. The receptor for advanced glycation end products (RAGE) sustains autophagy and limits apoptosis, promoting pancreatic tumor cell survival. Cell Death Differ 2010;17:666–76.
34. Bluemlein K, Gluckmann M, Gruning NM, Feichtinger R, Kruger A, Wamelink M, et al. Pyruvate kinase is a dosage-dependent regulator of cellular amino acid homeostasis. Oncotarget 2012;3:1356–69.
35. Dang CV. PKM2 tyrosine phosphorylation and glutamine metabolism signal a different view of the Warburg effect. Sci Signal 2009;2:pe75.
36. Dang CV. Links between metabolism and cancer. Genes Dev 2012; 26:877–90.
37. DeBerardinis RJ, Cheng T. Q's next: the diverse functions of glutamine in metabolism, cell biology and cancer. Oncogene 2010;29:313–24.
38. Yang C, Sudderth J, Dang T, Bachoo RM, McDonald JG, DeBerardinis RJ. Glioblastoma cells require glutamate dehydrogenase to survive impairments of glucose metabolism or Akt signaling. Cancer Res 2009;69:7986–93.
39. Wise DR, DeBerardinis RJ, Mancuso A, Sayed N, Zhang XY, Pfeiffer HK, et al. Myc regulates a transcriptional program that stimulates mitochondrial glutaminolysis and leads to glutamine addiction. Proc Natl Acad Sci U S A 2008;105:18782–7.
40. Vander Heiden MG. Targeting cancer metabolism: a therapeutic window opens. Nat Rev Drug Discov 2011;10:671–84.
41. Tomitsuka E, Kita K, Esumi H. An anticancer agent, pyrvinium pamoate inhibits the NADH-fumarate reductase system–a unique mitochondrial energy metabolism in tumour microenvironments. J Biochem 2012; 152:171–83.
42. Okamoto N, Miyagi Y, Chiba A, Akaike M, Shiozawa M, Imaizumi A, et al. Diagnostic modeling with differences in plasma amino acid profiles between non-cachectic colorectal/breast cancer patients and healthy individuals. Int J Med Med Sci 2009;1:1–8.
43. Tisdale MJ. Molecular pathways leading to cancer cachexia. Physiology 2005;20:340–8.
44. Choudry HA, Pan M, Karinch AM, Souba WW. Branched-chain amino acid-enriched nutritional support in surgical and cancer patients. J Nutr 2006;136:314S-8S.
45. Luo Y, Chihara Y, Fujimoto K, Sasahira T, Kuwada M, Fujiwara R, et al. High mobility group box 1 released from necrotic cells enhances regrowth and metastasis of cancer cells that have survived chemotherapy. Eur J Cancer 2013;49:741–51.
46. Sobin LH, Wittekind C, editors. UICC TNM Classification of malignant tumours. 6th ed. New York: John Wiley & Sons, Inc.; 2003.